5-1-1975

Heat and Moisture Conduction in Unsaturated Soils

J. A. Havens
University of Arkansas, Fayetteville

R. E. Babcock
University of Arkansas, Fayetteville

HEAT AND MOISTURE CONDUCTION IN UNSATURATED SOILS

by

J. A. Havens and R. E. Babcock

WATER RESOURCES RESEARCH CENTER
Publication No. 28

In Cooperation With The
ENGINEERING EXPERIMENT STATION

Research Report No. 25

UNIVERSITY OF ARKANSAS
Fayetteville
May 1975

PROJECT COMPLETION REPORT

PROJECT NO: A-014-ARK

ANNUAL ALLOTMENT

AGREEMENT NO: 14-31-0001-3804

Starting Date: June 1970

Completion Date: June 1974

HEAT AND MOISTURE CONDUCTION IN UNSATURATED SOILS

by

J. A. Havens and R. E. Babcock
Principal Investigators

ARKANSAS WATER RESOURCES RESEARCH CENTER
University of Arkansas
Fayetteville, Arkansas 72701

ACKNOWLEDGEMENT

The work performed during the contract period was supported in part with funds provided by the Office of Water Resources Research, U.S. Department of the Interior, under Grant Number A-014-ARK, as authorized under the Water Research Act of 1964, P.L. 88-379 as amended by P.L. 89-404 and P.L. 92-175.

The research was performed under the supervision of J. A. Havens and R. E. Babcock, Principal Investigators, by:

John H. Kendrick, Graduate Assistant

John L. Bondurant, Graduate Assistant

ABSTRACT

Mathematical models are developed for the prediction of heat transfer from hot water pipes buried in the soil. Heat transfer in the absence of moisture transfer is described as a function of the difference between the temperature of the pipe and the temperature of the soil surface. The energy balance is used to determine the longitudinal temperature distribution of the water. The method is extended to describe a system of equally spaced, parallel buried pipes. Soil temperature profiles around the pipes are presented. The model is used to calculate the land area that can be heated by an underground piping system carrying cooling water from the condensers of a 1000 MW nuclear-electric plant.

A new development of the phenomenological equations for coupled heat and moisture flow, based on the theory of Irreversible Thermodynamics, is presented. Solutionsof the equations for boundary conditions representative of buried piping systems designed for simultaneous soil heating and irrigation are presented.

TABLE OF CONTENTS

LIST OF FIGURES

I. INTRODUCTION

The beneficial use of "waste heat" from electric power generation facilities is receiving increased attention as a means of simultaneously reducing the thermal pollution threat to surface waters and "recovering" part of the valuable thermal energy rejected from power plant steam condensers. One such beneficial use is soil heating to increase agricultural crop production. Such an alternative to current power plant heat rejection practices may be advantageous where water reserves sufficient to prevent undesirable temperature increases are not available and where atmospheric conditions preclude the use of cooling towers for closed loop cooling. An added advantage could accrue from potential return on investment from increased crop yields in an integrated power-plant/agricultural complex.

Boersma (1) proposed an agricultural complex utilizing waste heat to enhance production of fresh or saltwater fish and crustaceans, to produce high protein food supplement in warm water ponds which use waste rejected from animal rearing facilities as raw material input, and to increase conventional crop production by soil heating.

The writers' work was initiated in response to a need for better design tools by which to study the practicality and cost-effectiveness of soil heating for agricultural purposes. Other investigators have predicted land area requirements for power plant heat rejection by soil

heating with grossly oversimplified mathematical models. These models, which perhaps give "order of magnitude" information useful for preliminary evaluation of soil heating, are not sufficiently accurate for design or even cost-study use.

The work performed under this contract can be divided into three areas.

1) A thorough literature survey was made to determine the present capability for predicting heat and moisture transfer through the soil-plant-atmosphere complex from subsurface conduits carrying warm water from power plant condensers. This survey included a study of mathematical models previously proposed for heat and/or mass transfer in soil (and to the atmosphere from the soil surface) as well as a survey of physical data required for such models. The latter include determinations of thermal conductivity, moisture (liquid and vapor) transfer coefficients (i.e. diffusivity), and heat capacity. Such measurements are very difficult in some cases, and therefore only scattered, incomplete data are to be found in the literature. This is particularly true for the effects on the aforementioned properties of such factors as surface tension (capillary effects), "coupled" heat and moisture flow, simultaneous liquid and vapor flow, and "history-dependence," all of which are common and may be important in the soil-water system.

2) Mathematical models were developed for predicting heat transfer from buried water pipes, by the method of images. The new models

allow for temperature variation of the water along the length of the pipe, and will predict two-dimensional temperature fields and accompanying heat transfer for systems of multiple, parallel, buried pipes. Unidirectional flow in all pipes as well as flow in alternate directions in neighboring pipes (useful for partial elimination of temperature gradients throughout the root zone) can be modeled. Although the models described require the assumption of constant soil-surface temperature and constant soil thermal properties, it is believed that they can be useful in design of subsurface soil warming systems when "average values" of thermal properties are used. The models allow prediction of land use requirements and provide a tool useful for optimizing the soil warming system design with respect to such parameters as pipe size, burial depth, horizontal spacing, and water flow rates.

3) The last phase of the work was the development of mathematical models for the description of simultaneous, "coupled," heat and moisture transfer in soil. The development is based on the methods of Irreversible Thermodynamics. Many investigators have studied unsaturated soil moisture flow in the presence of temperature gradients, but very little effort has been made to solve the resulting model equations with boundary conditions similar to those which would be anticipated in a simultaneous soil warming-irrigation complex. Furthermore, previous developments

in this area, particularly those based on the methods of Irreversible Thermodynamics, have not all been consistent with thermodynamics theory. It is believed that the development presented here of the so-called "phenomenological equations," which describe coupled energy and mass transfer, provides added insight into these processes. Although this phase of the work has not been completed because of unforseen problems which arose in the numerical solution of the equations, the group at the University of Arkansas Water Resources Research Center plans to continue this investigation on a non-funded basis.

BACKGROUND AND LITERATURE SURVEY

The growing demand for electric power is causing concern about the effect on the environment of the tremendous quantities of heat that must be rejected from steam generation power plant condensers. The temperature increase of condenser cooling water averages 15°F (1). The amount of water withdrawn from U.S. waterways for condenser cooling is estimated to be 40 trillion gallons per year, or roughly 10 percent of the total surface water flow in U.S. rivers and streams. The return of this heated water places a thermal burden of approximately five quadrillion Btu per year on the environment (1970 figures).

Many warm water utilization schemes have been proposed for beneficial use of reject heat from steam electric power plants. One such scheme, proposed by Boersma (2), involves the use of subsurface piping systems carrying the hot condenser water discharge to heat soil in agricultural complexes. Soil warming has two attractive benefits: extension of the growing season (sometimes allowing multiple cropping), and acceleration of plant growth.

As the first phase of the writers' work, a literature survey was made of methods applicable to the modeling of subsurface water-pipe soil heating system design and evaluation. Although none of the previously developed models were considered satisfactory, a very large body of literature bearing directly on the problem was identified. Only the more important examples of previous work which were associated directly with further work undertaken by the writers' group are dicussed herein. For purposes of convenience

as well as organization, the previous work is divided into two groups: (1) heat transfer only and (2) simultaneous heat and moisture transfer. In addition an extensive list of published literature surveyed which would be of interest to investigators in this field is included as Appendix I.

HEAT TRANSFER ALONE

The first published study of heat loss from buried pipes appears to have been by Allen (3) in 1920. Allen developed the following equation for determining heat loss:

$$\dot{q} = \frac{2\pi k\,(T_1 - T_2)}{\ln\,(r_2/R)} \qquad [1]$$

where

$\dot{q}$ = heat flow rate per unit length of pipe

T_1 = temperature of the outside of the pipe assumed equal to that of the fluid in the pipe

T_2 = average temperature of the ground at a point where the heat from the pipe does not affect the ground temperature appreciably

R = outside radius of the pipe

r_2 = distance from the center of the pipe at which the temperature of the ground becomes T_2

k = thermal conductivity of the ground.

Allen concluded from his studies that the heat loss from a buried pipe is not proportional to the external surface area of the pipe. He also stated that the burial depth makes little difference in the heat loss, provided the center of the pipe is two feet or more below the surface.

His model assumes an "infinitely extended isotropic, constant property soil and can be developed easily by use of an energy balance and Fourier's Law.

Karge (4) presented the following equation in 1945 for predicting the temperature drop in oil pipe lines:

$$\ln \frac{T_I - T_\alpha}{T - T_\alpha} = \frac{2\pi RUZ}{\dot{m}\, Cp} \qquad [2]$$

where

T = oil temperature at some distance Z down the line

T_I = initial temperature of the oil

T_α = atmospheric temperature

R = outside radius of the pipe

Z = length of pipe

Cp = heat capacity of the oil

$\dot{m}$ = flow rate of oil

U = heat transfer coefficient, oil to atmosphere.

Karge's model includes the effect of external surface area of the pipe.

A model essentially identical to Allen's (3) was proposed by Kemler and Oglesby (5) for use in heat pump design.

Andrews (6) described the "shape factor method" for predicting heat transfer in a solid with complicated boundary conditions. The shape factor is used in the equation:

$$\dot{q} = -k\ (S.F.)\ \Delta T \qquad [3]$$

where

$\dot{q}$ = heat flow rate

k = thermal conductivity of solid

ΔT = "characteristic" temperature difference

S.F. = geometrical shape factor.

Using the method of images and the principle of superposition, Andrews developed shape factors for heat transfer between neighboring cylinders and from a cylinder to an infinite plate. He used these shape factors to predict heat transfer between two pipes buried in the ground. Andrews' method did not account for the effect of the soil surface boundary condition. He did, however, suggest an iterative procedure to account for temperature gradients along the length of a pipe.

Carslaw (7), and more recently Jakob (8) and Kutateladze (9) used the method of images to calculate heat transfer from a buried pipe to the surrounding soil. Jakob (8) presented the following model for the temperature distribution in a homogeneous soil around a buried pipe or cable:

$$T(x,y) - T_s = \frac{\dot{q}}{4\pi k} \ln \frac{x^2 + (h-y)^2}{x^2 + (h+y)^2} \qquad [4]$$

where

$T(x,y)$ = temperature at any point in the soil

T_s = surface temperature of the soil

k = thermal conductivity of the soil

$\dot{q}$ = heat transfer rate per unit length of cable

h = depth of burial, measured to the center line of pipe or cable

x = horizontal distance from center of cable

y = vertical distance from soil surface.

This model assumes an isothermal soil surface whose temperature is controlled by external factors independent of the buried pipe temperature. (This assumption is discussed in Section V.)

The previous models were developed in all cases with the constraint that an analytic solution of the model was required. This requirement led to the assumptions of constant soil thermal properties, constant soil surface temperature (for the method of images), and one-dimensional or symmetrical temperature fields. The use of finite difference numerical methods designed for digital computer simulation allows treatment of variable thermal properties and more realistic boundary conditions. However, computer simulation of heat transfer from buried pipes does not seem to have been pursued to an appreciable extent, at least not in the published literature, before 1970. Furthermore, the increased modeling capability associated with such methods is gained at the expense of ease of computation and, perhaps more important, with some sacrifice of usefulness in cost optimization studies. Because a goal of the present work is to develop mathematical models useful for initial design and cost evaluation, as well as for use in optimizing design parameters, primary emphasis was given to "continuous" (as opposed to finite difference) models.

The primary deficiencies in the models previously suggested for prediction of heat transfer from buried pipes carrying warm water are

1) assumption of constant property, isotropic soil,
2) neglect of temperature variation along the length of the pipe, and
3) neglect (except in the "method of images" methods) of the effect of the soil surface boundary condition.

HEAT AND MOISTURE TRANSFER

It is well known that the "effective thermal conductivity" of soil increases with moisture content. The early attempts to modify heat transfer models for application to moist soils merely incorporated increased "average" thermal conductivity values. Schmill (10) used the method of images to determine the "effective" thermal conductivity of soil around a buried cable when moisture migration from the vicinity of the cable had occurred.

Field experiments by Boersma (2) demonstrated migration of moisture away from warm water lines buried in the ground. This moisture migration leads to the development of a "dry core" around the pipe with substantially reduced thermal conductivity and heat transfer. It appears at this time that the use of underground soil heating systems would be impractical without provision for simultaneous irrigation to prevent drying of the soil in the plant root zone. Thus, although pure heat transfer models with "average values" of thermal conductivity may be useful in determining estimates of the land area required for a given heat rejection from power plant condensers, models capable of predicting heat and mass transfer will almost certainly be required for a final system design.

The published literature on simultaneous heat and mass transfer is extensive. Attempts to model this kind of process have ranged from almost totally empirical to state-of-the-art theory. The most common approach is to combine the classical models of Fourier and Darcy. Philip and DeVries (11) proposed the following model.

Classical Model

The Philip and DeVries model describes moisture and heat transfer in porous media under combined moisture and temperature gradients. The model is said to apply in all ranges of moisture content:

$$q_\ell/\rho_\ell = -D_{\theta\ell}\nabla\theta_\ell - D_{T\ell}\nabla T - Ki$$

$$q_v/\rho_\ell = -D_{\theta v}\nabla\theta_\ell - D_{TV}\nabla T \qquad [5]$$

$$q_n = -(\lambda - L\rho_\ell D_{TV})\nabla T + Lq_v + C_\ell(T-T_o)q_m$$

where q_ℓ is the liquid flux, g/cm^{2}sec

$D_{\theta\ell}$ is the isothermal liquid diffusivity of water in soil, cm^2/sec

θ_ℓ is the volumetric water content, cm^3 of water/cm^3 of soil

$D_{T\ell}$ is the thermal liquid diffusivity, cm^2/sec°C

K is the unsaturated hydraulic conductivity, cm/sec

i is a unit vector in the vertical direction

q_v is the vapor flux, g/cm^{2}sec

ρ_ℓ is the density of liquid water, g/cm^3

$D_{\theta v}$ is the isothermal vapor diffusivity, cm^2/sec

D_{TV} is the thermal vapor diffusivity, cm^2/sec

q_n is the heat flux, cal/cm^{2}sec

λ is the thermal conductivity, cal/cm sec°C

L is the heat of vaporization, cal/g

C_ℓ is the specific heat capacity of liquid water, cal/g°C

T_o is an arbitrary reference temperature, °C

T is the temperature, °C

q_m is the total moisture flux = $q_\ell + q_v$, g/cm^{2}sec

∇ is the gradient operator.

The various diffusivity values are further given by DeVries (11) as:

$$D_{TV} = fD_{atm}\nu\beta h(\nabla T)_a/\rho_\ell \nabla T$$

where D_{atm} is the molecular diffusion coefficient of water vapor in air, cm^2/sec

ν is a mass flow factor, dimensionless

$\beta = d\rho_v/dT$, g/cm^3°C

ρ_ℓ is the density of saturated water vapor, g/cm^3

$(\nabla T)_a$ is the average temperature gradient in air-filled pores, °C/cm

$f = S$, $\theta_\ell < \theta_{\ell k}$

$f = a + a\theta_\ell/(S-\theta_{\ell k})$

a is the volumetric air content, cm^3 of air/cm^3 of soil

$\theta_{\ell k}$ is the value of θ_ℓ at which liquid continuity fails

S is the porosity .

$$D_{T\ell} = K\gamma\psi$$

where γ is the temperature coefficient of surface tension, 1/°C

ψ is the matric suction potential, cm.

$$D_{\theta\ell} = K\frac{\partial\psi}{\partial\theta_\ell}$$

$$D_{\theta v} = \alpha\, a\, D_{atm}\nu g\rho_v(\partial\psi/\partial\theta_\ell)/\rho_\ell RT$$

where α is a tortuosity factor for diffusion of gases in soil, dimensionless

g is the acceleration due to gravity, cm/sec^2

ρ_v is the density of water vapor, g/cm^3

R is the universal gas constant, erg/g°C.

This model ignores the coupling effects between the liquid phase moisture transfer and the vapor phase moisture transfer.

Equations [5], with appropriate boundary conditions, could be solved to predict heat and moisture transfer in a soil warming-irrigation system. However, measurement of the information required for specification of the diffusivity coefficient is difficult.

A model very similar to that proposed by Philip and DeVries can be "developed" by the method of Irreversible Thermodynamics (12, 13, 14). Cary and Taylor (12) presented the following model for simultaneous heat and moisture transfer in soil, using this method.

Irreversible Thermodynamic Model

Cary and Taylor (12) used the method of Irreversible Thermodynamics to develop equations describing the transfer of heat and mass in soil. The equations are applicable only in the high moisture content (liquid dominant) range:

$$J_w = -\rho D[\nabla\theta + \beta^*\nabla \ell nT]$$

$$J_q = -\rho D\beta\nabla\theta - L_{qq}\nabla \ell nT$$

where J_w is the liquid water flux, $g/cm^2 \cdot day$

J_q is the heat flux, $cal/cm^2 \cdot day$

θ is the volumetric water content, cm^3 of water/cm^3 of soil

L_{qq} is a phenomenological coefficient equal to the thermal conductivity of the soil multiplied by the temperature, cal/day·cm

T is the temperature, °K

D is the isothermal coefficient of diffusivity of liquid water in soil, cm^2/day

ρ is the density of the system, g/cm^3 (assumed constant)

β^* is a coefficient defined as $\nabla\theta/\nabla\ell nT$ at steady state and zero water flux, dimensionless

β is a coefficient defined as $\nabla\mu_w/\nabla\ell nT$ at steady state and zero water flux, cal/g

μ_w is the chemical potential of water, cal/g (assumed a single valued function of θ)

∇ is the gradient operator.

Both the Cary and Taylor and Philip and DeVries models have been tested in experimental studies involving frozen soil conditions (15), and evaporation from soil (16), and in sealed laboratory soil columns (17, 18). The general consensus in the literature seems to be that the Philip and DeVries model applies but the Cary and Taylor model does not. Most of the studies, however, were performed with fairly dry soils. A careful re-evaluation of one of the studies (18) indicated to the investigators that the Cary and Taylor model does predict moisture transfer under the influence of both moisture and temperature gradients. It should be noted that no independent measurements have been made of the heat flux in any of the experimental studies found, and the applicability of either model for prediction of the heat transfer has not been tested.

The principal investigator believes that the Cary and Taylor model, or a suitable modification thereof, can be used to predict heat and moisture transfer in unsaturated soils under conditions anticipated in subsurface soil warming-irrigation systems. However, a development of the phenomenological equations is presented which is believed to lend further insight into the model.

III. DEVELOPMENT OF THE MATHEMATICAL MODELS FOR HEAT TRANSFER

Consider an arbitrary length of water pipe buried at a constant depth in the soil. Assume that there is a temperature variation in the water in the longitudinal direction only. A steady-state energy balance written for the system defined by the outside boundary surface of the pipe and the ends of a small length of pipe, Z and Z + ΔZ, gives

$$\dot{m}\,\underline{H}\Big|_{Z}\;\Delta t - \dot{m}\;\underline{H}\Big|_{Z+\Delta Z}\;\Delta t + \dot{q}\Delta Z\Delta t = 0 \qquad (1)$$

where $\dot{m}$ = mass flow rate of water through the pipe

$\underline{H}$ = specific enthalpy of water crossing the boundary

$\dot{q}$ = heat flow rate per linear length unit at boundary of system

Z = coordinate on longitudinal axis

ΔZ = a small length of pipe

Δt = arbitrary length of time.

Equation (1) expresses the requirement that at steady state the net rate of heat transfer across the system boundary is equal to the net rate of energy transfer associated with mass flow across the system boundary.

Dividing Equation (1) by $\Delta Z\Delta t$, and taking the limit of the result as ΔZ approaches zero, gives

$$\dot{m}\,\frac{d\underline{H}}{dZ} + \dot{q} = 0. \qquad (2)$$

If the enthalpy of the fluid crossing the boundary is considered a function of temperature only, then

$$d \underline{H} = Cp \; d \; T_w \tag{3}$$

where Cp = heat capacity of water at temperature T_w

T_w = temperature of water at coordinate Z.

Using Equation (3), one can write Equation (2) as

$$\dot{m} \; Cp \; \frac{d \; T_w}{d \; Z} + \dot{q} = 0. \tag{4}$$

Equation (4) is the differential energy balance for any point in the system. If $\dot{q}$ can be described as a function of the temperature of the water in the pipe at any longitudinal position Z, Equation (4), with appropriate boundary conditions, can be solved for the longitudinal temperature distribution of the water in the pipe. The length of pipe which is required to transfer a given amount of heat to the surrounding soil thus can be determined.

CASE I:

Consider a single pipe buried in a homogeneous soil at a constant depth, h. Assume that the water in the pipe is at a temperature higher than that of the surrounding soil, that there is no temperature variation in the water in the radial direction, and that the temperature drop across the pipe wall is negligible. If the soil medium were infinite, the steady-state radial flow of heat, at any cross-section of the pipe, from the water into the soil would be described by Fourier's second law,

$$\frac{d}{dr} \left(rk \frac{dT}{dr} \right) = 0 \tag{5}$$

where k = thermal conductivity of the soil

r = radial distance from the pipe center

T = temperature of the medium at any radial distance r.

The boundary conditions are:

$$\dot{q} = \left(-2\pi r k \frac{dT}{dr}\right) \Big| r = R \qquad (6)$$

where R = outside radius of the pipe, and

$$T = T_w \quad \text{at } r = R. \qquad (7)$$

If one assumes that the thermal conductivity of the soil is independent of temperature, Equation (5) becomes a linear, ordinary differential equation and can be solved by standard techniques. The integrated form of Equation (5) for the stated boundary conditions is

$$T - T_w = \frac{-\dot{q}}{2\pi k} \ln (r/R). \qquad (8)$$

Equation (8) is invalid for points in a semi-infinite soil medium. However, it can be modified to describe the case of semi-infinite soil by the method of images (8). Refer to Figure 1. The method consists of supposing the soil medium to be infinitely extended. The pipe is represented by a line source of heat, located at the centerline of the pipe, with the same heat strength, $\dot{q}$, as that of the pipe at the cross-section. A plane of constant temperature, Ts, at a distance h from the line source, is simulated by the superimposition of the effect of a line source of heat strength $-\dot{q}$ reflected symmetrically to the desired isothermal plane. The system is now an unbounded soil medium with a heat source, a heat

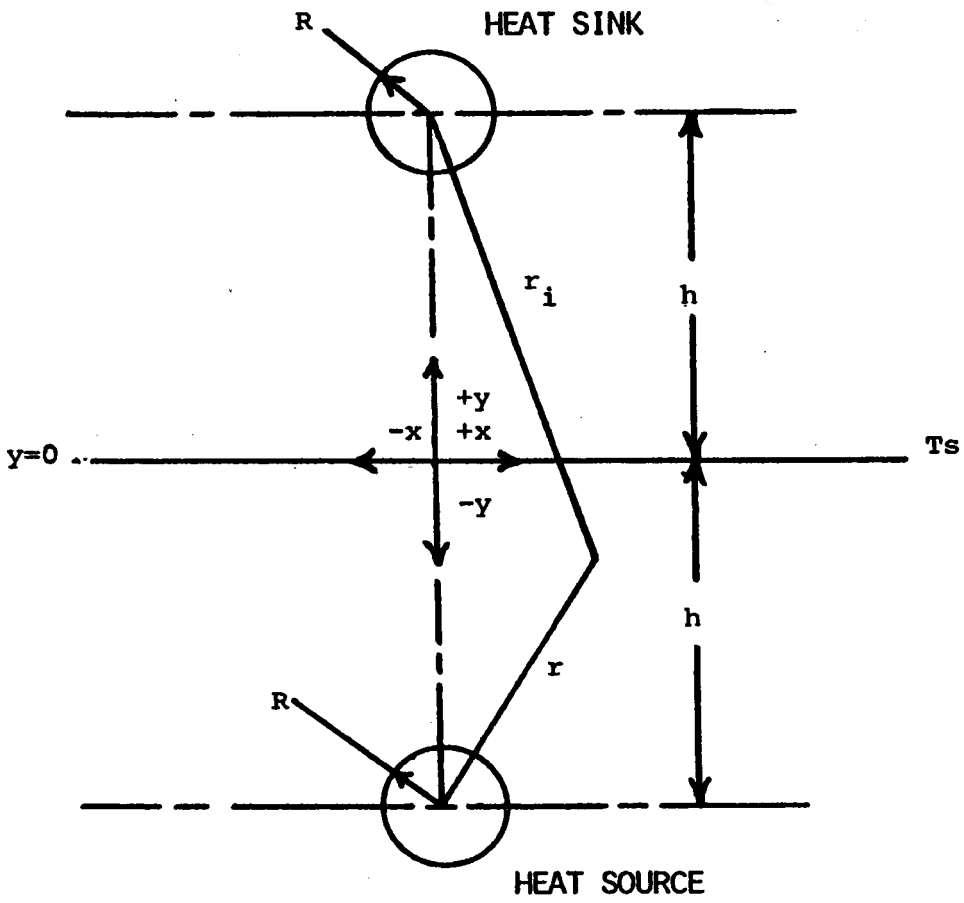

Figure 1 Configuration Of Heat Source And Fictitious Heat Sink (Image) For Determination Of Temperature Distribution Around A Buried Pipe By Method Of Images

sink, and an isothermal plane representing the surface of the ground. The effect of the superposition of the heat sink is to cancel any temperature variation at the plane y = 0 which results from the temperature contribution of the positive source.

It is convenient to transform the temperature scale so that Ts is the zero temperature point. Mathematically, this transformation is represented as

$$\Theta = T - Ts \tag{9}$$

where Θ = temperature excess above or below the soil surface temperature.

Equation (8) can be written as

$$\Theta' - \Theta_w = \frac{-\dot{q}}{2\pi k} \ln (r/R) \tag{10}$$

where Θ_w = temperature excess of the water above the soil surface temperature (T_w - Ts).

The "prime" indicates that the temperature excess is due to the source without presence of the sink.

The temperature field which would be established by the heat sink alone is described by the negative of Equation (10),

$$\Theta_i' - \Theta_{wi} = \frac{+\dot{q}}{2\pi k} \ln (r_i/R) \tag{11}$$

where Θ_i' = the temperature excess at radial distance r_i

Θ_{wi} = temperature excess at $r_i = R$

r_i = radial distance from image heat sink.

Summing the separate temperature fields represented by

Equations (10) and (11) gives

$$\Theta = T - Ts = \frac{\dot{q}}{2\pi k} \ln (r_i/r) \qquad (12)$$

Noting that $r_i = \sqrt{x^2 + (h-y)^2}$, and that $r = \sqrt{x^2 + (h+y)^2}$, one can write Equation (12) as

$$T_{(x,y)} - Ts = \frac{\dot{q}}{2\pi k} \ln \sqrt{\frac{x^2 + (h-y)^2}{x^2 + (h+y)^2}} \qquad (13)$$

where x = horizontal distance from source or sink

h = distance from soil surface to source

(h+y)= vertical distance from source

(h-y)= vertical distance from image sink.

Temperatures calculated from Equation (13) for points inside the radius r = R have no physical meaning because it is assumed initially that there is no temperature variation in the water in the radial direction.

The temperature calculated at the point (0,-h+R) approximates the water temperature. This temperature is, from Equation (13),

$$T_w = Ts + \frac{\dot{q}}{2\pi k} \ln \left(\frac{2h-R}{R}\right). \qquad (14)$$

It is important to note that $\dot{q}$ is not constant along the length of the pipe.

Equation (14) may be solved for $\dot{q}$,

$$\dot{q} = \frac{2\pi k \ (T_w - Ts)}{\ln \left(\frac{2h-R}{R}\right)}. \qquad (15)$$

Substituting $\dot{q}$ from Equation (15) into Equation (4) yields

$$\dot{m}Cp \frac{d(T_w-Ts)}{dz} + \frac{2\pi k (T_w-Ts)}{\ln (\frac{2h-R}{R})} = 0. \quad (16)$$

Equation (16) is a first order ordinary differential equation. The initial condition is

$$T_w = T_I \quad \text{at} \quad Z = 0 \quad (17)$$

where T_I = initial water temperature.

Solving Equation (16) by standard techniques yields

$$T_w = Ts + (T_I-Ts) \exp\left[\frac{-2\pi kZ}{\dot{m}Cp \ln(\frac{2h-R}{R})}\right] \quad (18)$$

or, solving for Z,

$$Z = \frac{\ln\left(\frac{T_I-Ts}{T_w-Ts}\right) \dot{m}Cp \ln (\frac{2h-R}{R})}{2\pi k}. \quad (19)$$

For a required temperature drop of the water, the necessary length of pipe can be calculated from Equation (19).

CASE II:

Consider a system of equally spaced parallel pipes, all buried at the same depth below the surface of a homogeneous soil. The arrangement is illustrated in Figures 2-a and 2-b. There are N pipes on either side of the center pipe, for a total of (2N+1) pipes in the system, all having the same radius R. Water flows in the same direction at equal velocity in all pipes. The center pipe in the layout is taken for analysis.

Because Equation (13) is the solution to an ordinary, linear differential equation with linear boundary conditions,

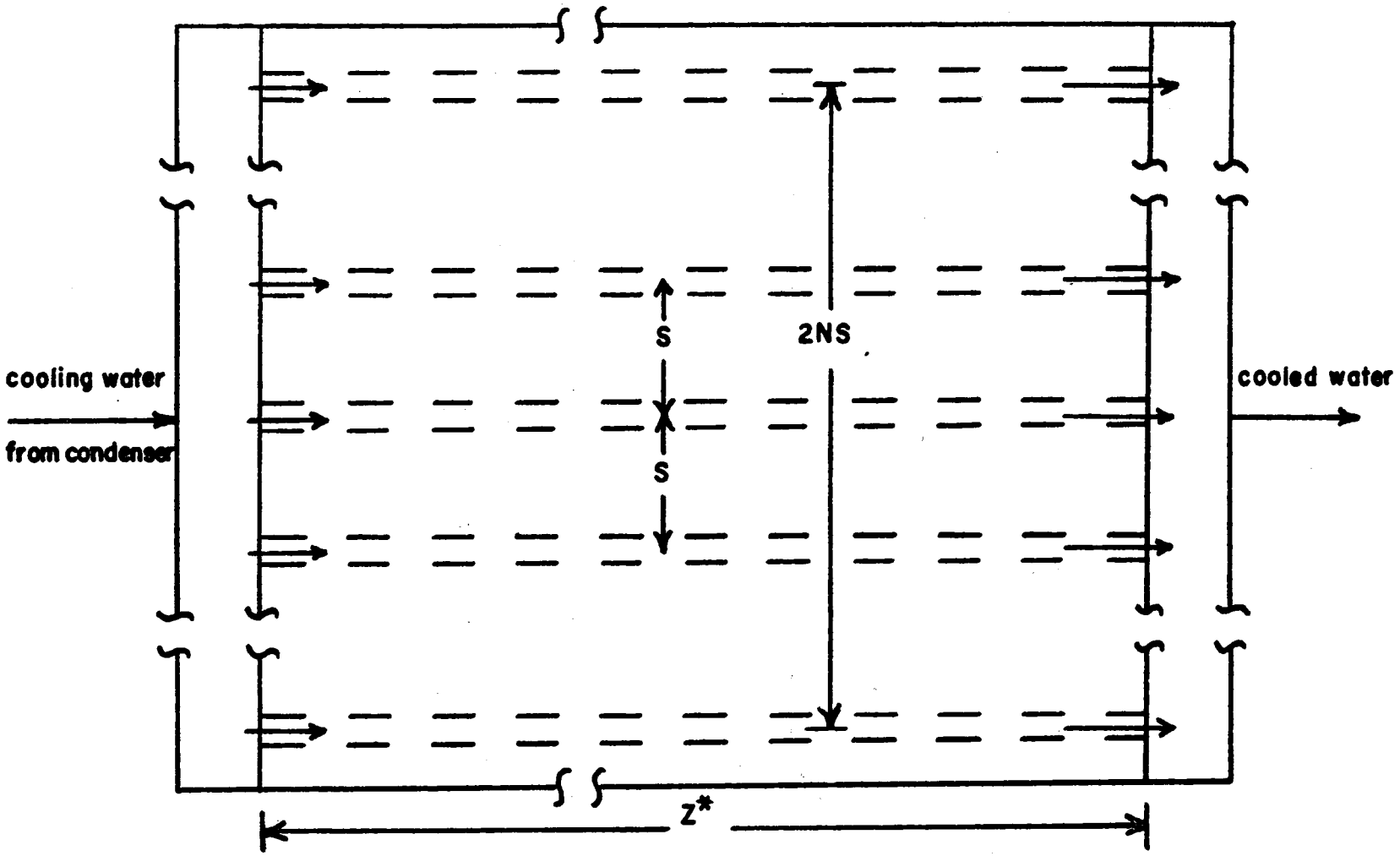

Figure 2-a Top View Of Soil Warming System With Water Flowing In The Same Direction In Neighboring Pipes

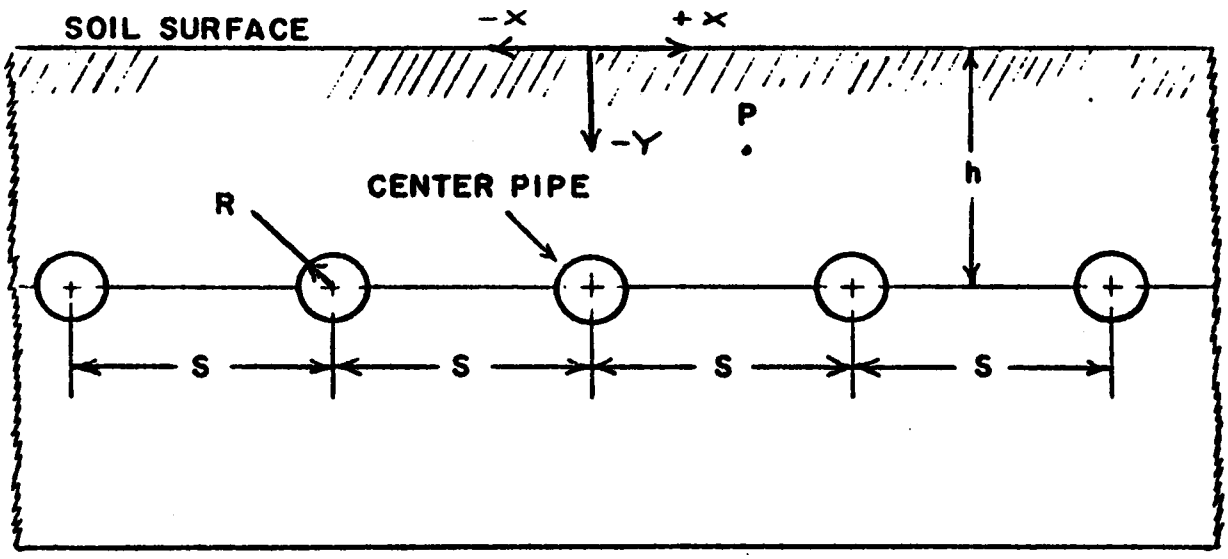

Figure 2-b Cross-Sectional View Of Soil Warming System With Water Flowing In The Same Direction In Neighboring Pipes

the temperature field established by each pipe (considered to be a line source) at an arbitrary cross-section is independent of all the other pipes (line sources) in the field. Thus, the effects of all sources can be superimposed to determine the temperature at a given point. The temperature field established by a single source was derived in CASE I (Equation (13)).

The temperature established at an arbitrary point P (refer to Figure 2-b) by the nth source (numbered from the center source) on the positive x-direction side is

$$T_{(x,y)} - Ts = \frac{\dot{q}}{2\pi k} \ln \sqrt{\frac{(nS-x)^2 + (h-y)^2}{(nS-x)^2 + (h+y)^2}} \qquad (20)$$

where (nS-x) = the horizontal distance from the source to point P

S = lateral distance between sources.

The temperature established at point P by the nth source on the negative x-direction side is

$$T_{(x,y)} - Ts = \frac{\dot{q}}{2\pi k} \ln \sqrt{\frac{(nS+x)^2 + (h-y)^2}{(nS+x)^2 + (h+y)^2}} \qquad (21)$$

where (nS + x) = the horizontal distance from the source to point P.

All sources are of the same heat strength $\dot{q}$. Superimposition of the fields established by all the sources, at point P, yields

$$T_{(x,y)} - Ts = \frac{\dot{q}}{2\pi k} \left[\ln \sqrt{\frac{x^2 + (h-y)^2}{x^2 + (h+y)^2}} + \sum_{n=1}^{N} \ln \sqrt{\frac{(nS-x)^2 + (h-y)^2}{(nS-x)^2 + (h+y)^2}} + \sum_{n=1}^{N} \ln \sqrt{\frac{(nS+x)^2 + (h-y)^2}{(nS+x)^2 + (h+y)^2}} \right]. \qquad (22)$$

As in CASE I, the temperature at the point (0,-h+R) approximates the water temperature. This temperature is, from Equation (22),

$$T_w = Ts + \frac{\dot{q}}{2\pi k}\left[\ln\frac{2h-R}{R} + \sum_{n=1}^{N}\ln\frac{(nS)^2+(2h-R)^2}{(nS)^2+R^2}\right]. \qquad (23)$$

It should be noted that all sources were taken to be of equal heat strength. The logarithmic series in Equation (23) converges rapidly. For a large number of pipes, the equal source strength analysis is a valid simulation for all pipes except those very near the sides of the field. The variation in the boundary area pipes can be ignored without significant error for the application considered here.

Equation (23) can be solved for $\dot{q}$,

$$\dot{q} = \frac{2\pi k\,(T_w-Ts)}{\left[\ln\left(\frac{2h-R}{R}\right) + \sum_{n=1}^{N}\ln\left(\frac{(nS)^2+(2h-R)^2}{(nS)^2+R^2}\right)\right]}. \qquad (24)$$

Substituting $\dot{q}$ from Equation (24) into Equation (22) yields

$$T_{(x,y)}-Ts = \frac{(T_w-Ts)}{\left[\ln\left(\frac{2h-R}{R}\right) + \sum_{n=1}^{N}\ln\left(\frac{(nS)^2+(2h-R)^2}{(nS)^2+R^2}\right)\right]}$$

$$\left[\ln\sqrt{\frac{x^2+(h-y)^2}{x^2+(h+y)^2}} + \sum_{n=1}^{N}\ln\sqrt{\frac{(nS-x)^2+(h-y)^2}{(nS-x)^2+(h+y)^2}} + \sum_{n=1}^{N}\ln\sqrt{\frac{(nS+x)^2+(h-y)^2}{(nS+x)^2+(h+y)^2}}\right]. \qquad (25)$$

Equation (25) can be used to calculate the temperature at any point in the cross-section, with the exception of points inside a circle of radius R around each source. Temperatures inside

these circles have no physical meaning because of the initial assumption of no temperature variation in the water in the radial direction.

Substituting $\dot{q}$ from Equation (24) into Equation (4) yields

$$\dot{m}Cp \frac{d(T_w-Ts)}{dz} + \frac{2\pi k (T_w-Ts)}{\left[\ln\left(\frac{2h-R}{R}\right) + \sum_{n=1}^{N} \ln\left(\frac{(nS)^2+(2h-R)^2}{(nS)^2+R^2}\right)\right]} = 0. \quad (26)$$

This is a first order ordinary differential equation. The initial condition is the same as in CASE I,

$$T_w = T_I \qquad \text{at} \qquad Z = 0. \quad (17)$$

Solving Equation (25) by standard techniques yields

$$T_w = Ts + (T_I-Ts) \exp\left[\frac{-2\pi kZ}{\dot{m}Cp\left[\ln\left(\frac{2h-R}{R}\right) + \sum_{n=1}^{N} \ln\left(\frac{(nS)^2+(2h-R)^2}{(nS)^2+R^2}\right)\right]}\right] \quad (27)$$

or, solving for Z,

$$Z = \frac{1}{2\pi k} \ln\left(\frac{T_I-Ts}{T_w-Ts}\right)\dot{m}Cp \left[\ln\left(\frac{2h-R}{R}\right) + \sum_{n=1}^{N} \ln\left(\frac{(nS)^2+(2h-R)^2}{(nS)^2+R^2}\right)\right]. \quad (28)$$

For a required temperature drop of the water, Equation (27) can be solved for the necessary length of pipe. By ignoring the variation in the boundary area pipes, one obtains the total area heated,

$$\text{AREA} = 2NSZ^* \quad (29)$$

where Z^* = length of pipe necessary to drop the water temperature a required amount.

CASE III:

Consider a system of equally spaced parallel pipes, all buried at the same depth below the surface of a homogeneous soil. There is a total of (2N + 1) pipes in the system, all having the same radius R. Water flows in opposite directions, at equal velocity, in neighboring pipes. The arrangement is illustrated in Figures 3-a and 3-b. In Figure 3-b, the symbols H and C represent the relative temperatures of the water in each pipe at an arbitrary cross-section. The center H and C pipes are taken for analysis.

The H and C pipes in the system are simulated by line sources of heat strength $\dot{q}_1$ and $\dot{q}_2$, respectively. As in CASE II, the temperature field established by each source is independent of all other sources. Thus, the contributions of all sources at a given cross-section to the temperature at an arbitrary point can be superimposed to determine the temperature at that point. The temperature field established by a single source was derived in CASE I (Equation 13).

The temperature established at point P (referring to Figure 3-b) by the nth H source in the positive x-direction (numbered from the center H source) is

$$T_{(x,y)} - Ts = \frac{\dot{q}_1}{2\pi k} \ln \sqrt{\frac{(h-y)^2 + (2nS-x)^2}{(h+y)^2 + (2nS-x)^2}} \qquad (30)$$

where (2nS-x) = the horizontal distance from the nth H source to point P

(h+y) = the vertical distance from the nth H source to point P.

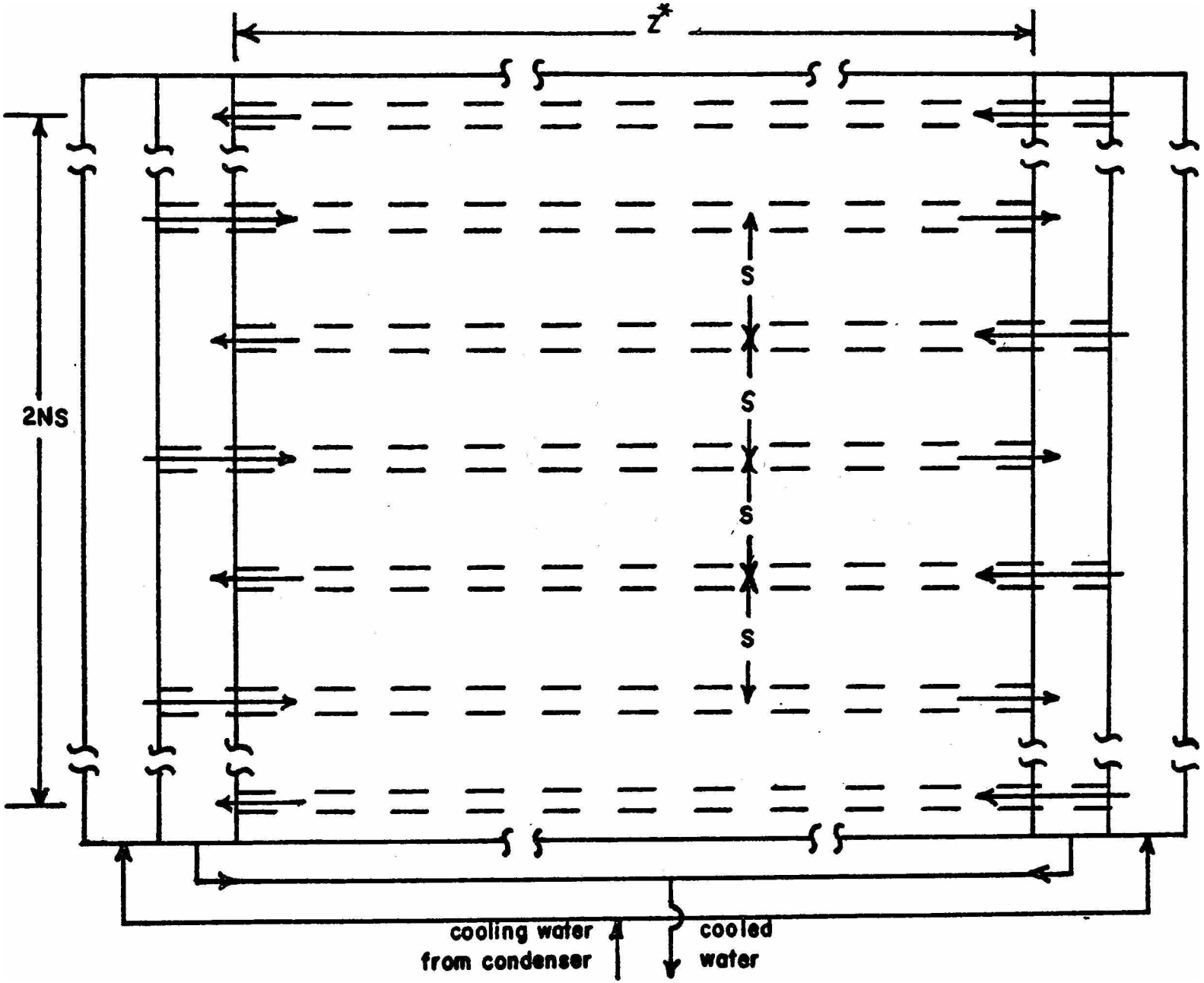

Figure 3-a Top View Of Soil Warming System With Water Flowing In Opposite Directions In Neighboring Pipes

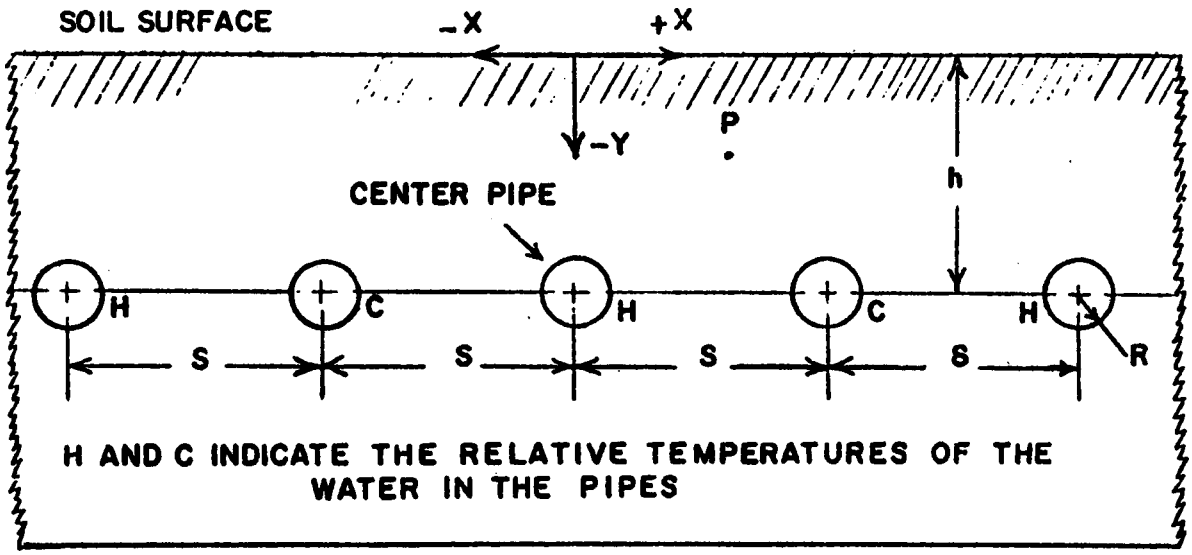

Figure 3-b Cross-Sectional View Of Soil Warming System With Water Flowing In Opposite Directions In Neighboring Pipes

The temperature established at point P by the nth H source in the negative x-direction is

$$T_{(x,y)} - Ts = \frac{\dot{q}_1}{2\pi k} \ln \sqrt{\frac{(h-y)^2 + (2nS + x)^2}{(h+y)^2 + (2nS + x)^2}} \qquad (31)$$

where (2nS + x) = the horizontal distance from the nth H source to point P.

The temperature established at point P by the nth C source in the positive x-direction is

$$T_{(x,y)} - Ts = \frac{\dot{q}_2}{2\pi k} \ln \sqrt{\frac{(h-y)^2 + (2nS-S-x)^2}{(h+y)^2 + (2nS-S-x)^2}} \qquad (32)$$

where (2nS-S-x) = the horizontal distance from the nth C source to point P.

The temperature established at point P by the nth C source in the negative x-direction is

$$T_{(x,y)} - Ts = \frac{\dot{q}_2}{2\pi k} \ln \sqrt{\frac{(h-y)^2 + (2nS-S+x)^2}{(h+y)^2 + (2nS-S+x)^2}} \qquad (33)$$

where (2n-S+x) = the horizontal distance from the nth C source to point P.

Superimposition of all temperature fields established by the sources, at point P, yields

$$T_{(x,y)} - Ts = \frac{\dot{q}_1}{2\pi k} \left[\ln \sqrt{\frac{x^2+(h-y)^2}{x^2+(h+y)^2}} + \sum_{n=1}^{N/2} \ln \sqrt{\frac{(h-y)^2+(2nS-x)^2}{(h+y)^2+(2nS-x)^2}} \right.$$

$$\left. + \sum_{n=1}^{N/2} \ln \sqrt{\frac{(h-y)^2+(2nS+x)^2}{(h+y)^2+(2nS+x)^2}} \right] + \frac{\dot{q}_2}{2\pi k} \left[\sum_{n=1}^{N/2} \ln \sqrt{\frac{(h-y)^2+(2nS-S-x)^2}{(h+y)^2+(2nS-S-x)^2}} + \right.$$

$$+ \sum_{n=1}^{N/2} \ln \sqrt{\frac{(h-y)^2 + (2nS-S+x)^2}{(h+y)^2 + (2nS-S+x)^2}} \Bigg]. \qquad (34)$$

It should be noted that all H sources were taken to be of equal heat strength, and that all C sources were taken to be of equal strength. For a large number of pipes, this is a valid simulation for all pipes except those near the sides of the field, because all the logarithmic series in Equation (34) converge rapidly. The variation in the boundary area pipes can be ignored without significant error for the application considered here.

Application of Equation (34) to the point (0, -h + R) yields

$$(T_{w1}-Ts) = \frac{\dot{q}_1}{2\pi k} \left[\ln \left(\frac{2h-R}{R}\right) + \sum_{n=1}^{N/2} \ln \frac{(2h-R)^2+(2nS)^2}{R^2 + (2nS)^2} \right]$$

$$+ \frac{\dot{q}_2}{2\pi k} \left[\sum_{n=1}^{N/2} \ln \frac{(2h-R)^2+(2nS-S)^2}{R^2 + (2nS-S)^2} \right] \qquad (35)$$

where T_{w1} = temperature of water in H pipe.

Application of Equation (34) to the point (S, -h + R) yields

$$(T_{w2}-Ts) = \frac{\dot{q}_2}{2\pi k} \left[\ln \left(\frac{2h-R}{R}\right) + \sum_{n=1}^{N/2} \ln \frac{(2h-R)^2+(2nS)^2}{R^2 + (2nS)^2} \right]$$

$$+ \frac{\dot{q}_1}{2\pi k} \left[\sum_{n=1}^{N/2} \ln \frac{(2h-R)^2+(2nS-S)^2}{R^2 + (2nS-S)^2} \right] \qquad (36)$$

where T_{w2} = temperature of water in C pipe.

Let

$$A = \left[\ln \left(\frac{2h-R}{R}\right) + \sum_{n=1}^{N/2} \ln \frac{(2h-R)^2+(2nS)^2}{R^2 + (2nS)^2} \right] \tag{37}$$

and

$$B = \sum_{n=1}^{N/2} \ln \frac{(2h-R)^2+(2nS-S)^2}{R^2 + (2nS-S)^2} . \tag{38}$$

Equations (35) and (36) then can be written, respectively, as

$$(T_{w1} - Ts) = \frac{\dot{q}_1}{2\pi k} A + \frac{\dot{q}_2}{2\pi k} B \tag{39}$$

and

$$(T_{w2} - Ts) = \frac{\dot{q}_2}{2\pi k} A + \frac{\dot{q}_1}{2\pi k} B . \tag{40}$$

These equations can be solved simultaneously for $\dot{q}_1$ and $\dot{q}_2$. The result is

$$\dot{q}_1 = \frac{2\pi k \left[A(T_{w1}-Ts) - B (T_{w2}-Ts)\right]}{A^2 - B^2} \tag{41}$$

and

$$\dot{q}_2 = \frac{2\pi k \left[A (T_{w2} - Ts) - B (T_{w1} - Ts)\right]}{A^2 - B^2} . \tag{42}$$

Substitution of $\dot{q}_1$ and $\dot{q}_2$ from Equations (41) and (42) into Equation (34) yields

$$T_{(x,y)} - Ts = \left[\frac{A (T_{w1}-Ts) - B (T_{w2}-Ts)}{A^2 - B^2}\right]\left[\ln \sqrt{\frac{x^2 + (h-y)^2}{x^2 + (h+y)^2}} + \sum_{n=1}^{N/2} \ln \sqrt{\frac{(h-y)^2+(2nS-x)^2}{(h+y)^2+(2nS-x)^2}} + \sum_{n=1}^{N/2} \ln \sqrt{\frac{(h-y)^2+(2nS+x)^2}{(h+y)^2+(2nS+x)^2}}\right]$$

$$+ \left[\frac{A (T_{w2}-Ts) - B(T_{w1}-Ts)}{A^2 - B^2}\right]\left[\sum_{n=1}^{N/2} \ln \sqrt{\frac{(h-y)^2+(2nS-S-x)^2}{(h+y)^2+(2nS-S-x)^2}} + \right.$$

$$+ \sum_{n=1}^{N/2} \ln \sqrt{\frac{(h-y)^2+(2nS-S+x)^2}{(h+y)^2+(2nS-S+x)^2}} \Bigg] . \qquad (43)$$

Equation (43) can be used to calculate the temperature at any point in the cross-section, with the exception of points inside a circle of radius R around each source. Temperatures inside these circles have no physical meaning because of the initial assumption of no temperature variation in the water in the radial direction.

Substituting $\dot{q}_1$ and $\dot{q}_2$ from Equations (41) and (42), respectively, into Equation (4) yields

$$\dot{m}Cp \frac{d(T_{w1}-Ts)}{dz} + \frac{2\pi k \left[A(T_{w1}-Ts) - B(T_{w2}-Ts) \right]}{A^2 - B^2} = 0 \qquad (44)$$

and

$$-\dot{m}Cp \frac{d(T_{w2}-Ts)}{dz} + \frac{2\pi k \left[A(T_{w2}-Ts) - B(T_{w1}-Ts) \right]}{A^2 - B^2} = 0 . \qquad (45)$$

The initial conditions are

$$T_{w1} = T_I \quad \text{at} \quad Z = 0 \qquad (46)$$

and

$$T_{w2} = T_F \quad \text{at} \quad Z = 0. \qquad (47)$$

Because of the symmetrical layout of the soil warming system,

$$T_{w1} = T_F \quad \text{at} \quad Z = Z^* \qquad (48)$$

and

$$T_{w2} = T_I \quad \text{at} \quad Z = Z^* \qquad (49)$$

where Z^* = length of pipe required to drop the water temperature from T_I to T_F.

The minus sign on the first term in Equation (45) is due to the fact that the mass flow in the pipe is in the opposite direction of the mass flow used in the derivation of Equation (4).

Laplace Transforming of Equations (44) and (45) and rearranging give , respectively,

$$f(s)\left[s + \frac{2\pi kA}{\dot{m}Cp(A^2-B^2)}\right] = (T_I-Ts) + \frac{2\pi kB}{\dot{m}Cp(A^2-B^2)}\,g(s) \quad (50)$$

and

$$g(s)\left[s - \frac{2\pi kA}{\dot{m}Cp(A^2-B^2)}\right] = (T_F-Ts) - \frac{2\pi kB}{\dot{m}Cp(A^2-B^2)}\,f(s) \quad (51)$$

where $f(s)$ = Laplace Transform of $(T_{w1}-Ts)$

$g(s)$ = Laplace Transform of $(T_{w2}-Ts)$

s = Transformation variable.

Solving these equations simultaneously for $f(s)$ and $g(s)$ yields

$$f(s) = \frac{(T_I-Ts)\left(s-\frac{2\pi kA}{\dot{m}Cp(A^2-B^2)}\right) + (T_F-Ts)\frac{2\pi kB}{\dot{m}Cp(A^2-B^2)}}{s^2 - \left(\frac{2\pi k}{\dot{m}Cp}\sqrt{\frac{1}{A^2-B^2}}\right)^2} \quad (52)$$

and

$$g(s) = \frac{(T_F-Ts)\left(s + \frac{2\pi kA}{\dot{m}Cp(A^2-B^2)}\right) - (T_I-Ts)\frac{2\pi kB}{\dot{m}Cp(A^2-B^2)}}{s^2 - \left(\frac{2\pi k}{\dot{m}Cp}\sqrt{\frac{1}{A^2-B^2}}\right)^2}. \quad (53)$$

Inversion of Laplace Transforms $f(s)$ and $g(s)$ gives, respectively,

$$T_{w1}-Ts = (T_I-Ts)\cosh\left(\frac{2\pi kZ}{\dot{m}Cp}\sqrt{\frac{1}{A^2-B^2}}\right) + \left[\frac{B(T_F-Ts)-A(T_I-Ts)}{A^2-B^2}\right] \sinh\left(\frac{2\pi kZ}{\dot{m}Cp}\sqrt{\frac{1}{A^2-B^2}}\right) \quad (54)$$

and

$$T_{w2}-Ts = (T_F-Ts)\cosh\left(\frac{2\pi kZ}{\dot{m}Cp}\sqrt{\frac{1}{A^2-B^2}}\right)+\left[\frac{A(T_F-Ts)-B(T_I-Ts)}{A^2-B^2}\right]$$

$$\sinh\left(\frac{2\pi kZ}{\dot{m}Cp}\sqrt{\frac{1}{A^2-B^2}}\right). \qquad (55)$$

The graph of Equation (55) is the translation by Z* of the mirror image of the graph of Equation (54) between the limits of Z=0 and Z*.

For a required temperature drop, Equation (54) or Equation (55) must be solved by trial and error for Z*. By ignoring the variation in the boundary area pipes, one obtains the total area heated,

$$AREA = 2NSZ^* . \qquad (56)$$

IV. APPLICATION OF MATHEMATICAL MODELS FOR HEAT TRANSFER

To calculate the land area that can be heated by an underground piping system carrying cooling water from the condensers of a 1000 megawatt nuclear-powered steam generation electric power plant, it is necessary to specify the physical conditions under which the system is to operate. For purposes of illustration, the following conditions are assumed.

1. The thermal efficiency of the power plant is 34 per cent.
2. The cooling water flow rate from the condensers is 39.6 million gallons per hour.
3. The cooling water is discharged from the condensers at a temperature of 100^{o}F.
4. The cooling water must be cooled to a temperature of 80^{o}F before it is returned to its natural origin.
5. The underground piping system consists of two-inch diameter pipes. The pipe wall thermal conductivity is large compared to the soil thermal conductivity. The pipes are buried at a depth of two feet and are spaced three feet apart.
6. The average velocity of the water in each pipe is five feet per second.
7. The thermal conductivity of the soil to be heated is 1.0 Btu/ft.-hr.-^{o}F.

The total number of pipes in the system can be calculated by dividing the total water flow rate by the water flow rate capacity of a single pipe. The total number of pipes is 2N+1, where

N is the number of pipes on either side of the center pipe in the field. Therefore

$$(2N+1) = \frac{\text{Total Water Flow Rate}}{\text{Water Flow Rate per Pipe}}$$

$$= \frac{(3.96 \times 10^7 \text{ gal/hr})(1 \text{ ft}^3/7.48 \text{ gal})(62.1 \text{ lbm/ft}^3)}{\left(\frac{\pi \cdot 1.0 \text{ in}^2}{144 \text{ in}^2/\text{ft}^2}\right)\left(5.0 \frac{\text{ft}}{\text{sec-pipe}}\right)(3600 \text{ sec/hr})(62.1 \text{ lb/ft}^3)}$$

$$= \frac{3.29 \times 10^8 \text{ lbm/hr}}{2.44 \times 10^4 \text{ lbm/hr-pipe}}$$

$$= 13{,}500 \text{ pipes.}$$

The total land area heated can be calculated by using the results of CASE II or CASE III.

CASE II: The water flows in the same direction in all pipes (see Figure 2-a). The length of the center pipe can be calculated from Equation (28):

$$Z^* = \frac{\ln\left(\frac{100^\circ\text{F}-64^\circ\text{F}}{80^\circ\text{F}-64^\circ\text{F}}\right)(2.44 \times 10^4 \text{ lbm/hr})(1.0 \text{ Btu/lbm } ^\circ\text{F})}{2\pi\ (1.0 \text{ Btu/ft.-hr.-}^\circ\text{F})}$$

$$\left[\ln\left(\frac{4.0-0.0833}{0.0833}\right) + \sum_{n=1}^{6750} \ln\frac{(3n)^2+(4.0-0.0833)^2}{(3n)^2+(0.0833)^2}\right]$$

$$= 18{,}400 \text{ feet.}$$

The total area heated is:

$$\text{AREA} = 2NSZ^* = \frac{2(6750)(3.0 \text{ ft})(18{,}400 \text{ ft})}{(43{,}560 \text{ ft}^2/\text{acre})}$$

$$= 17{,}095 \text{ acres.}$$

The longitudinal temperature profile of the water in the pipe is given by Equation (27):

$$T_w = 64.0\ ^{o}F + (36.0\ ^{o}F)\ \exp\ (-4.48 \times 10^{-5}\ Z).$$

The longitudinal water temperature profile is shown in Figure 4.

The temperature of the soil at any point in a given cross-section can be calculated from Equation (25). The corresponding water temperature at that cross-section to be used in Equation (25) can be obtained from Figure 4. Figures 5,6, and 7 are graphic representations of Equation (25) at longitudinal distances of 0, 7400, and 18,400 feet, respectively. In these figures, soil isotherms are plotted versus x and y.

As can be seen from Figures 5,6, and 7, the temperature distribution in the soil varies from one end of the field to the other. This variation is shown in Figure 8, a plot of the average temperature of the soil one foot below the surface of the ground versus longitudinal position in the field. The maximum and minimum temperatures of the soil at the one foot level also are shown in Figure 8.

CASE III: The water flows in opposite directions in neighboring pipes (see Figure 3-a). The length of the center pipe can be calculated from Equation (54) or Equation (55):

$$A = \ln\left(\frac{4.0-0.0833}{0.0833}\right) + \sum_{n=1}^{3375} \ln \frac{(4.0-0.0833)^2+(6n)^2}{(0.0833)^2+(6n)^2}$$

$$= 4.464$$

$$B = \sum_{n=1}^{3375} \ln \frac{4.0-0.0833)^2+(6n-3)^2}{(0.0833)^2=(6n-3)^2}$$

$$= 1.365$$

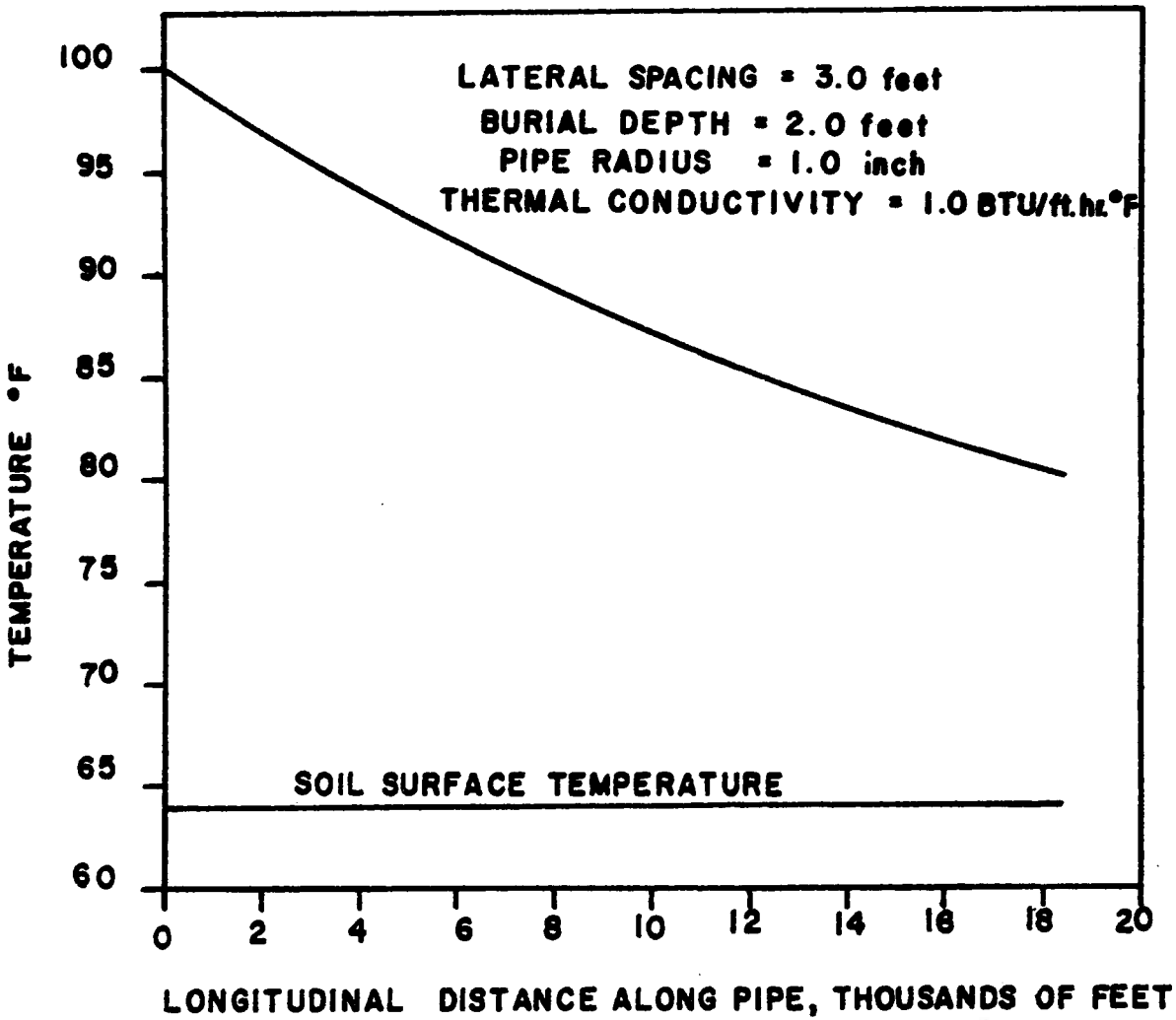

Figure 4 Longitudinal Temperature Profile Of Water In Pipe Of Soil Warming System With Water Flowing In The Same Direction In Neighboring Pipes

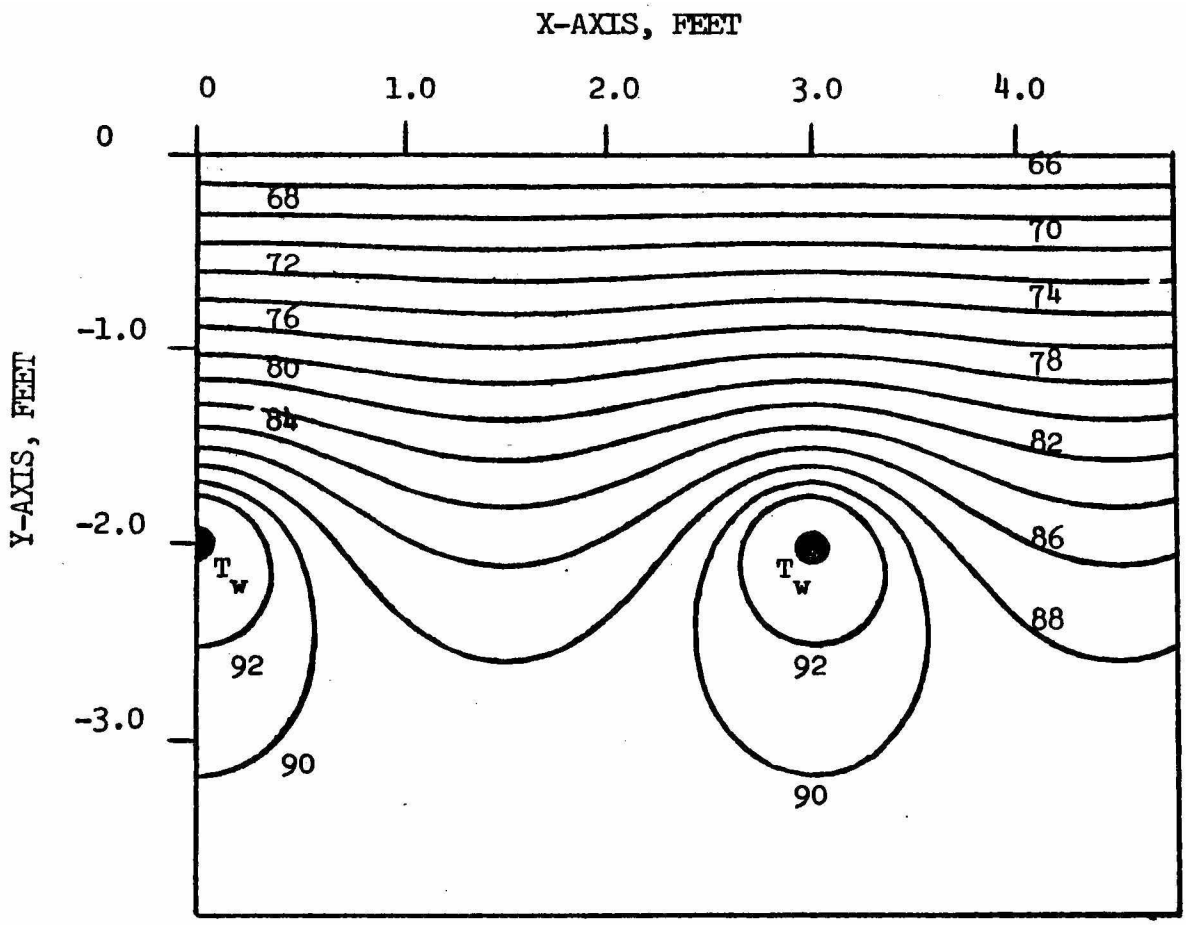

Figure 5 Soil Temperature Profiles At Z = 0 Feet Around Buried Pipes Of Soil Warming System With Water Flowing In The Same Direction In Neighboring Pipes

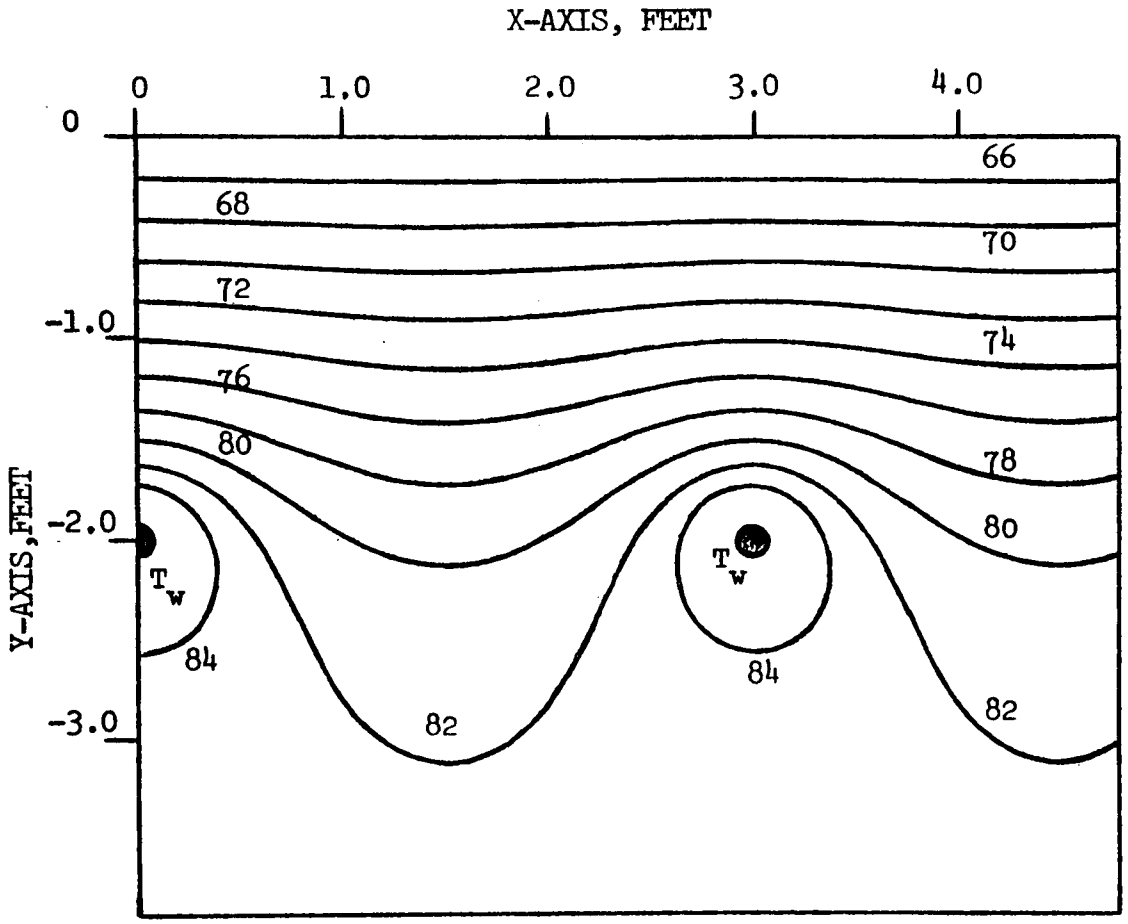

● INDICATES PIPE LOCATION

T_w = 90°F, T_s = 64°F

THERMAL CONDUCTIVITY = 1.0 Btu/hr.-ft.-°F
PIPE RADIUS = 1.0 inch

Figure 6 **Soil Temperature Profiles At Z = 7400 Feet Around Buried Pipes Of Soil Warming System With Water Flowing In The Same Direction In Neighboring Pipes**

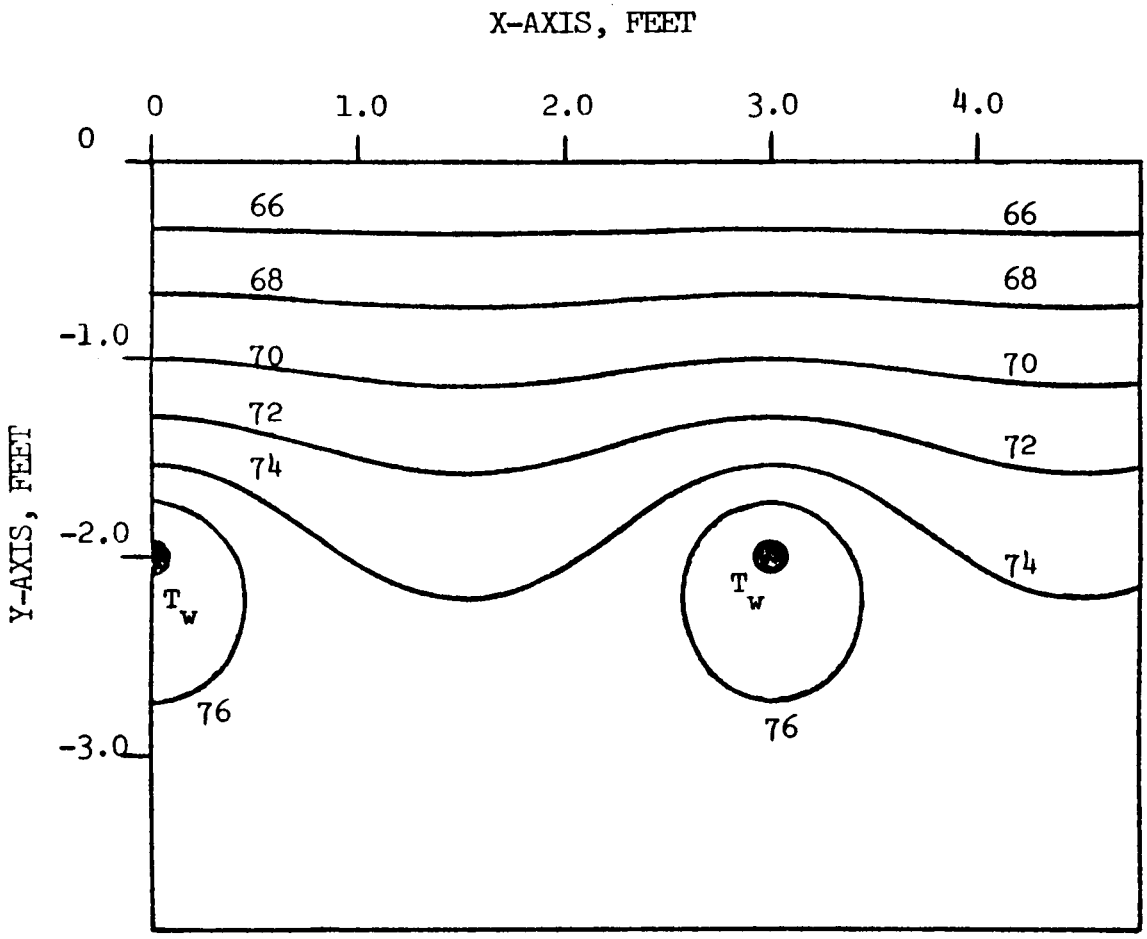

● INDICATES PIPE LOCATION

T_w = 80°F, T_s = 64°F

THERMAL CONDUCTIVITY = 1.0 Btu/hr.-ft.-°F
PIPE RADIUS = 1.0 inch

Figure 7 Soil Temperature Profiles At Z = 18,400 Feet Around Buried Pipes Of Soil Warming System With Water Flowing In The Same Direction In Neighboring Pipes

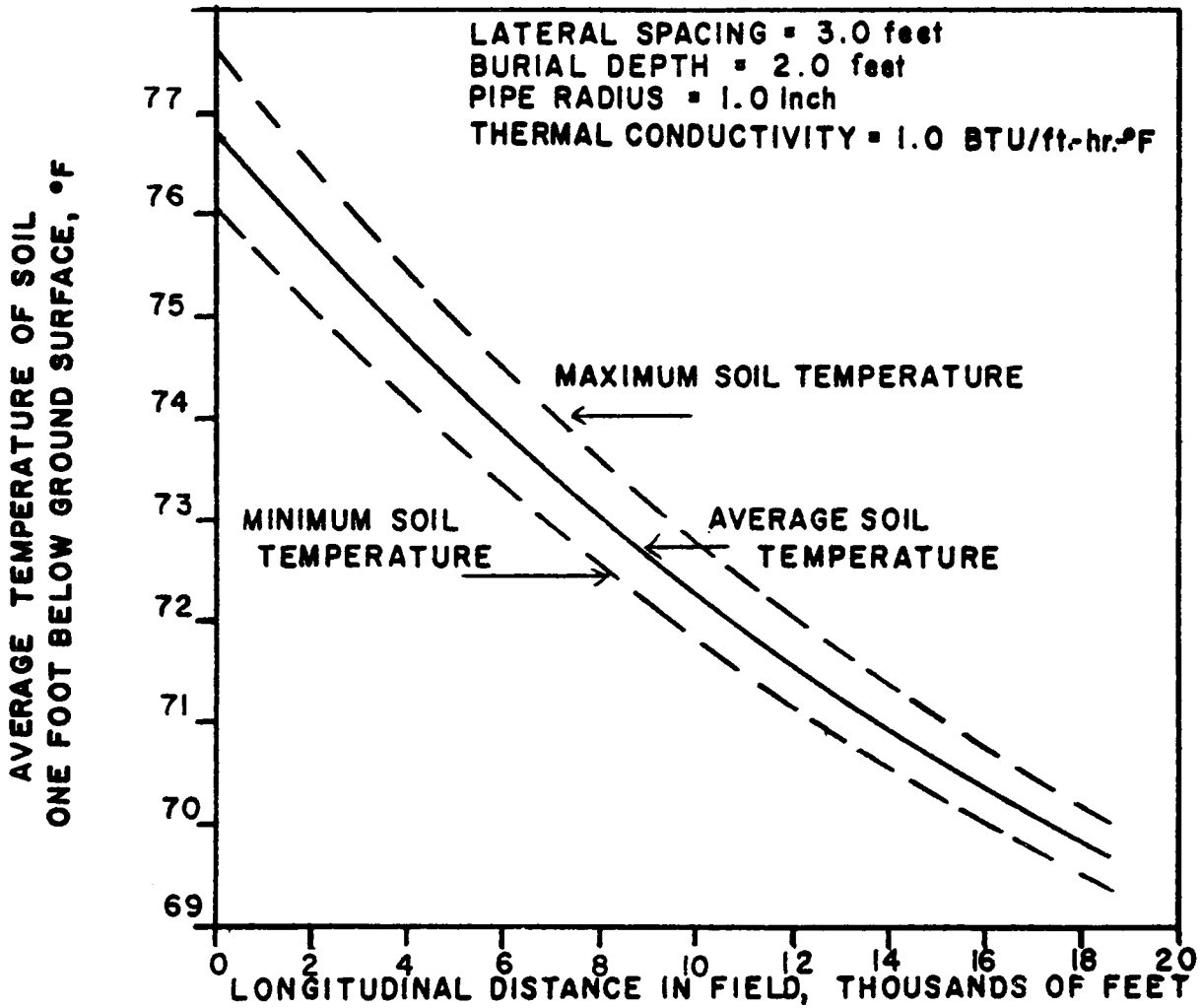

Figure 8 Temperature Variation One Foot Below Ground Surface Of Soil Warmed By A System Of Pipes With Water Flowing In The Same Direction In Neighboring Pipes

$$(80^{\circ}F-64^{\circ}F) = (100^{\circ}F-64^{\circ}F) \cosh (6.05 \times 10^{-5}Z^*)$$

$$+\left(\frac{1.365(80^{\circ}F-64^{\circ}F)-4.464\ (100^{\circ}F-64^{\circ}F)}{4.255}\right) \sinh (6.05 \times 10^{-5}Z^*) .$$

Solving for Z*, by trial and error,

$$Z^* = 19{,}360 \text{ feet} .$$

The total area heated is:

$$\text{AREA} = 2NSZ^* = \frac{2(6570)(3.0 \text{ ft})(19{,}360 \text{ ft})}{(43{,}560 \text{ ft}^2/\text{acre})}$$

$$= 18{,}035 \text{ acres} .$$

The longitudinal temperature profiles of the water in neighboring pipes are given by Equations (54) and (55):

$$T_{w1} = 64.0^{\circ}F+(36.0^{\circ}F) \cosh (6.05 \times 10^{-5}Z)$$
$$- (32.64^{\circ}F) \sinh (6.05 \times 10^{-5}Z)$$

$$T_{w2} = 64.0^{\circ}F + (16.0^{\circ}F) \cosh (6.05 \times 10^{-5}Z)$$
$$- (5.24^{\circ}F) \sinh (6.05 \times 10^{-5}Z).$$

The longitudinal water temperature profiles in neighboring pipes are shown in Figure 9.

The temperature of the soil at any point of a given cross-section of the field can be calculated from Equation (43). The corresponding water temperatures at that cross-section, to be used in Equation (43), can be obtained from Figure 9. Figures 10, 11, 12, and 13 are graphic representations of Equation (43) at longitudinal distances of 0, 6000, 9680, and 19,360 feet. In these figures, soil isotherms are plotted versus x and y.

As can be seen from Figures 10, 11, 12, and 13, the temperature distribution in the soil varies from one end of the field to

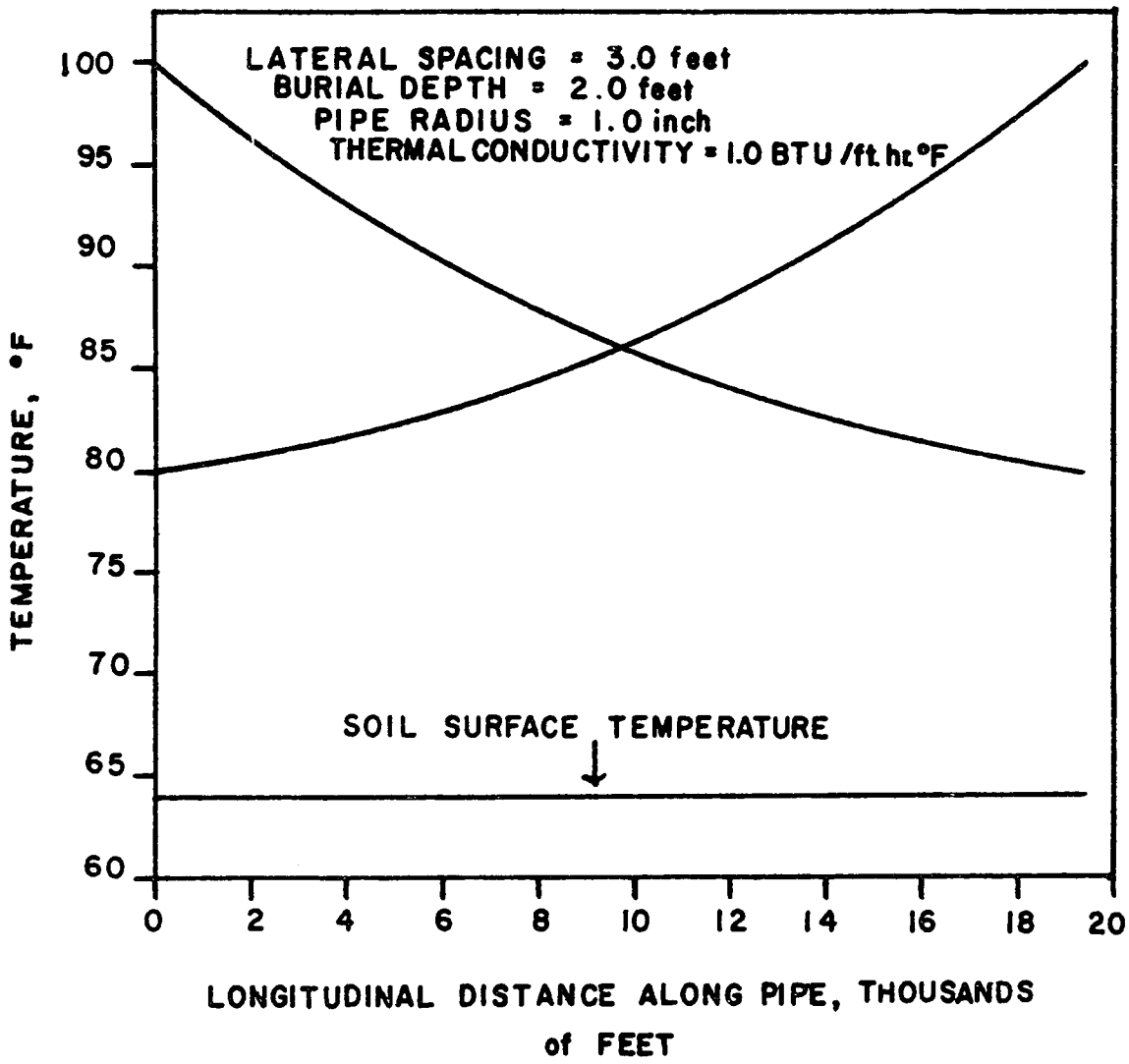

Figure 9 Longitudinal Temperature Profile Of Water In Adjacent Pipes Of Soil Warming System With Water Flowing In Opposite Directions In Neighboring Pipes

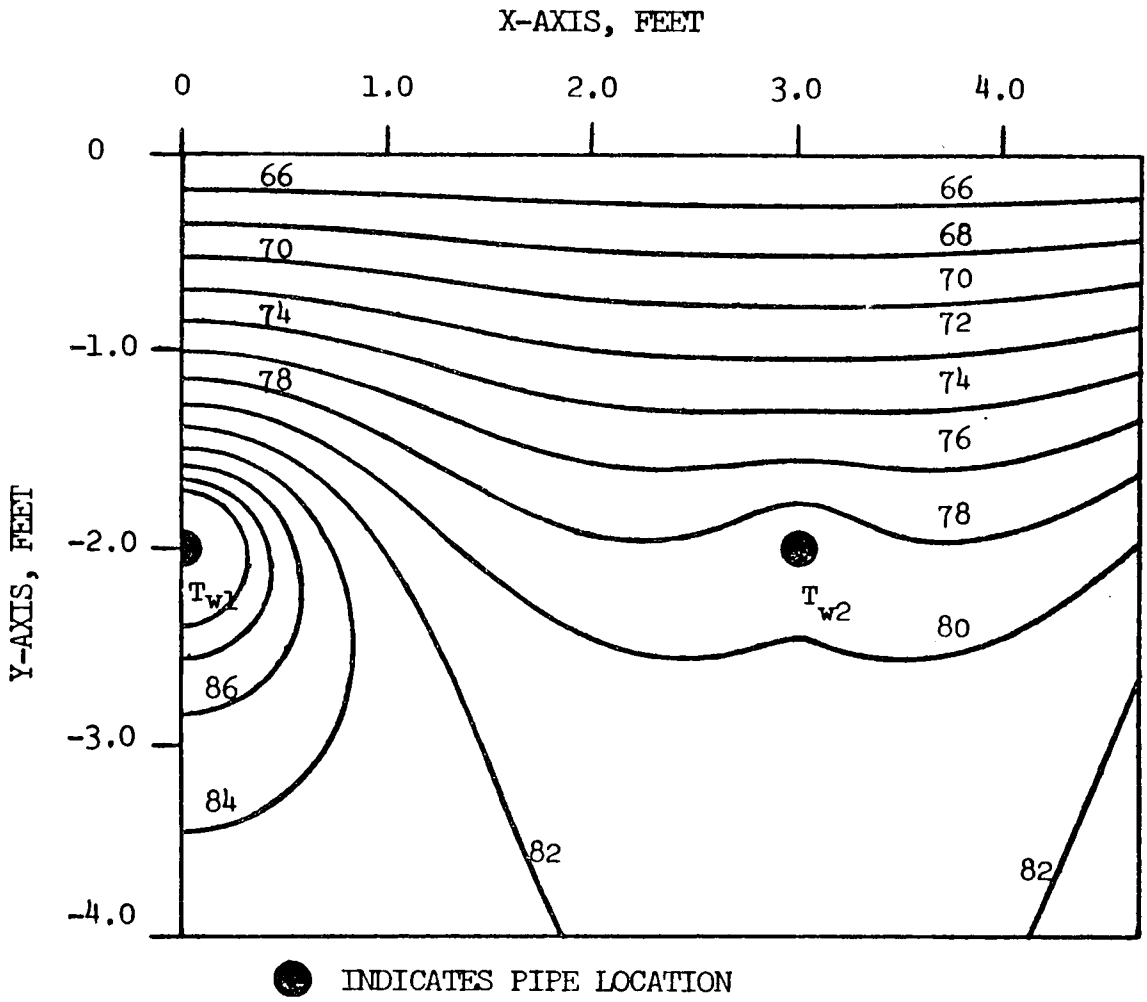

● INDICATES PIPE LOCATION

T_{w1} = 100°F, T_{w2} = 80°F, T_s = 64°F

THERMAL CONDUCTIVITY = 1.0 Btu/hr.-ft.-°F
PIPE RADIUS = 1.0 inch

Figure 10 Soil Temperature Profiles At Z = 0 Feet Around Buried Pipes Of Soil Warming System With Water Flowing In Opposite Directions In Neighboring Pipes

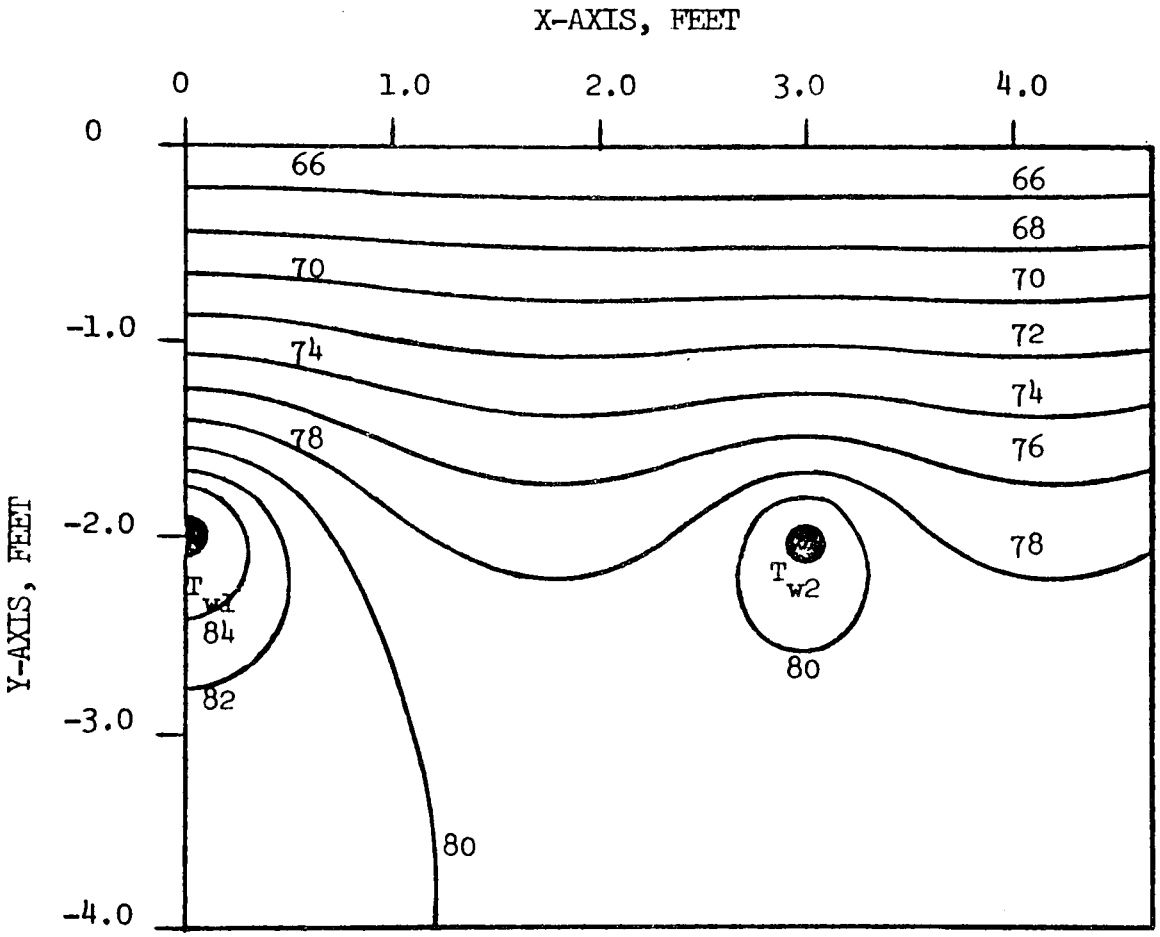

INDICATES PIPE LOCATION

T_{w1} = 90.275°F, T_{w2} = 82.999°F, T_s = 64°F

THERMAL CONDUCTIVITY = 1.0 Btu/ft.-hr.-°F
PIPE RADIUS = 1.0 inch

Figure 11 Soil Temperature Profiles At Z = 6000 Feet Around Buried Pipes Of Soil Warming System With Water Flowing In Opposite Directions In Neighboring Pipes

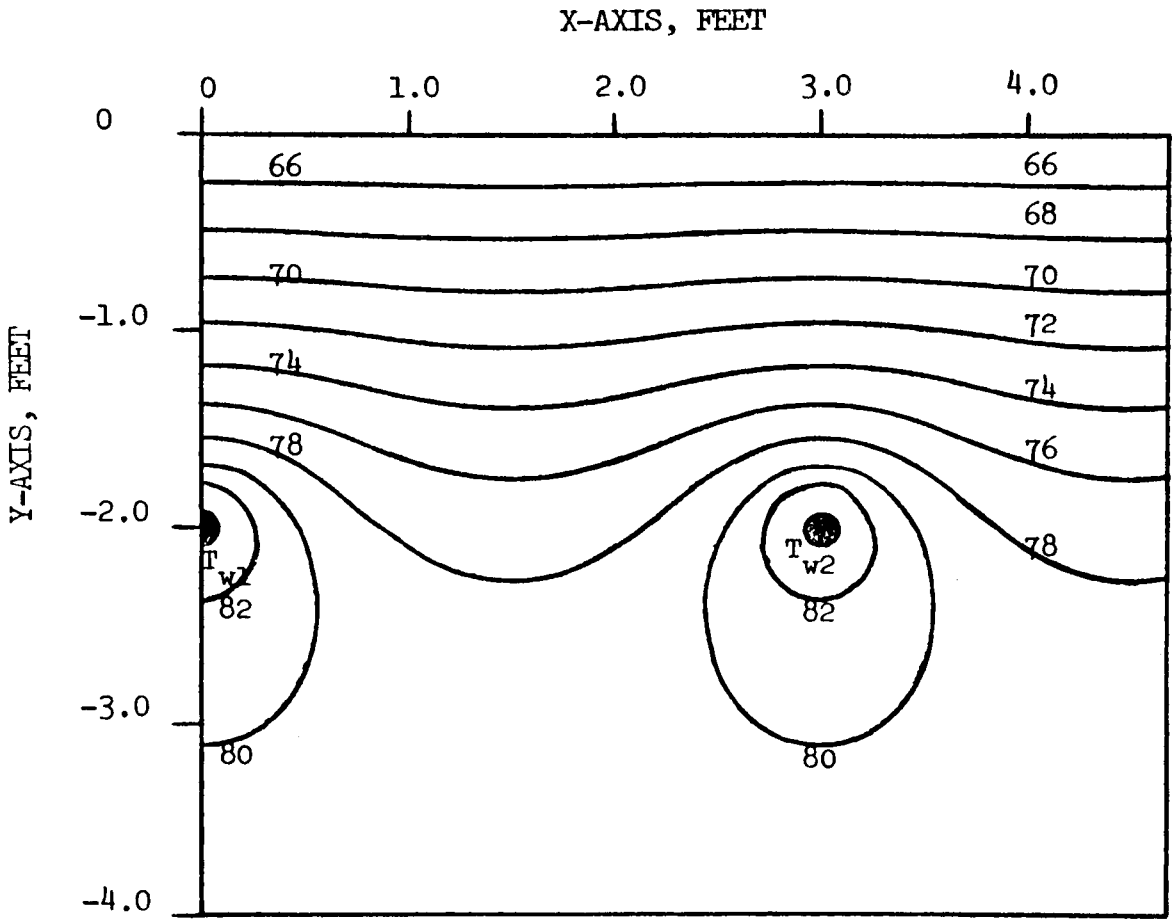

● INDICATES PIPE LOCATION

$T_{w1} = T_{w2} = 86.075°F$, $T_s = 64°F$

THERMAL CONDUCTIVITY = 1.0 Btu/ft.-hr.-°F
PIPE RADIUS = 1.0 inch

Figure 12 Soil Temperature Profiles At Z = 9680 Feet Around Buried Pipes Of Soil Warming System With Water Flowing In Opposite Directions In Neighboring Pipes

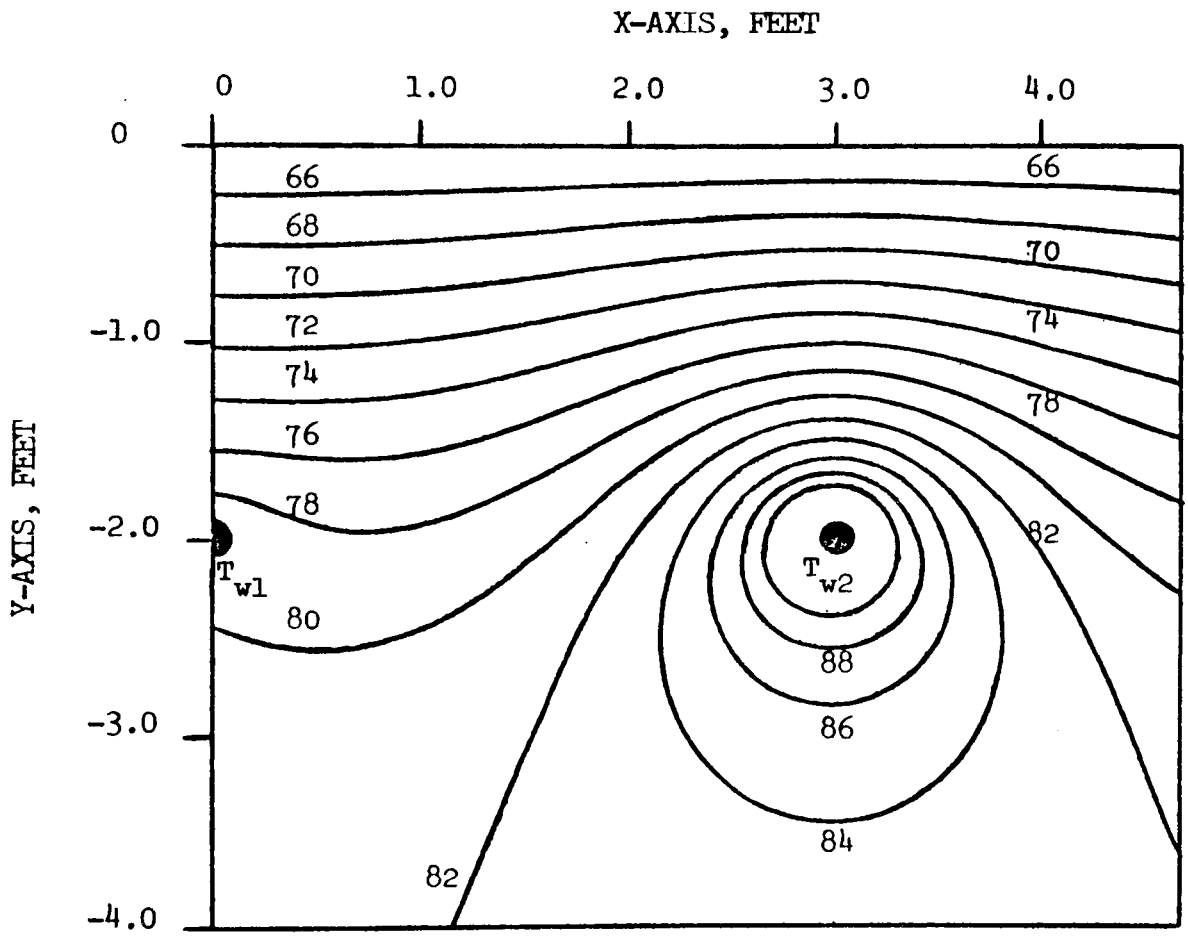

● INDICATES PIPE LOCATION

T_{w1} = 80°F, T_{w2} = 100°F, T_s = 64°F

THERMAL CONDUCTIVITY = 1.0 Btu/ft.-hr.-°F
PIPE RADIUS = 1.0 inch

Figure 13 Soil Temperature Profiles At Z = 19,360 Feet Around Buried Pipes Of Soil Warming System With Water Flowing In Opposite Directions In Neighboring Pipes

the other. This variation is shown in Figure 14, a plot of the average temperature of the soil one foot below the surface of the ground versus longitudinal position in the field. The maximum and minimum temperatures of the soil at the one foot level also are shown in Figure 14.

Figures 15, 16, 17, and 18 show the effect of burial depth, lateral spacing, pipe radius, and soil thermal conductivity, respectively, on the total land area heated by cooling water from the condensers of a 1000 megawatt nuclear-powered steam generation electric power plant, for the CASE II and CASE III soil warming systems.

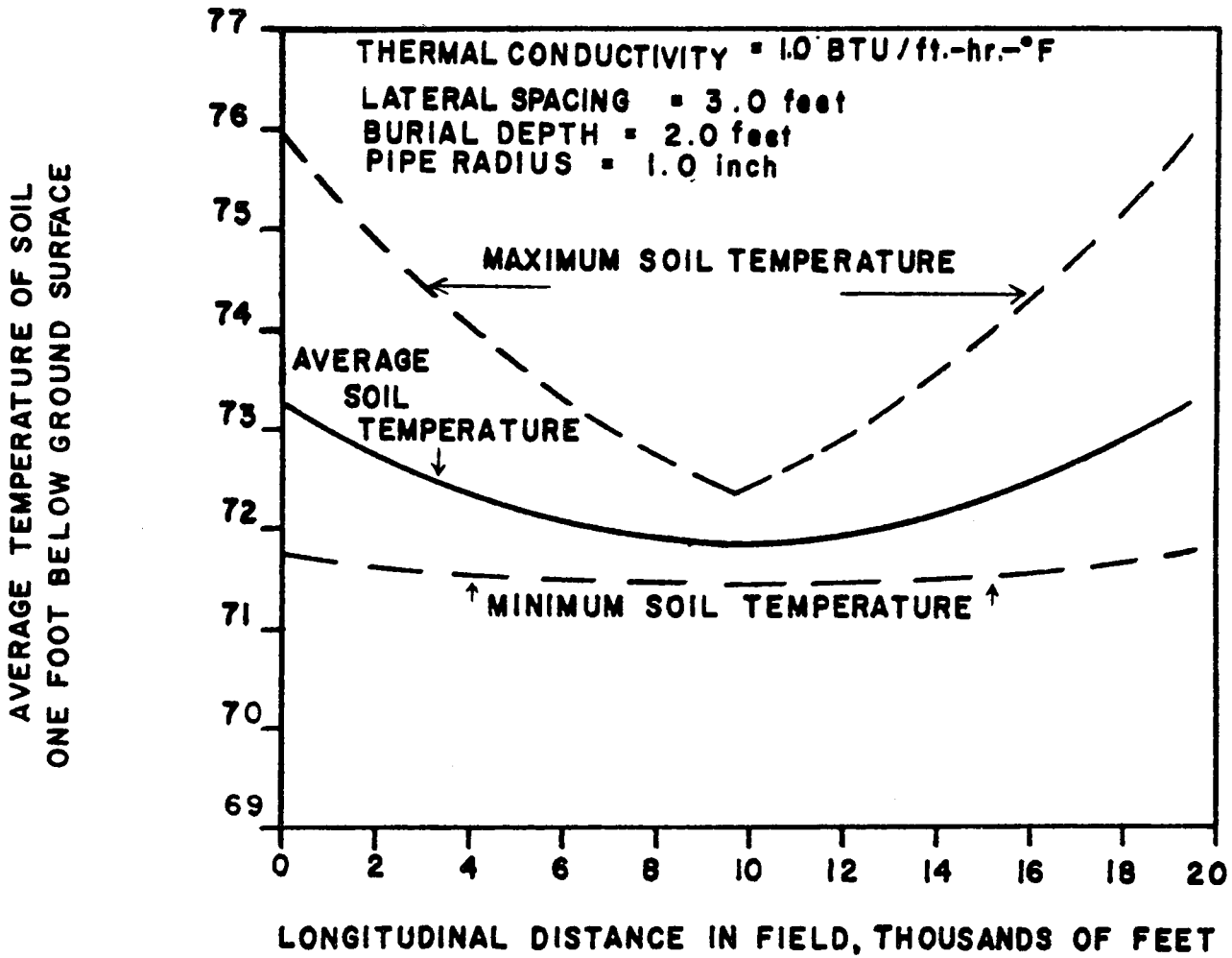

Figure 14 Temperature Variation One Foot Below Ground Surface Of Soil Warmed By A System Of Pipes With Water Flowing In Opposite Directions In Neighboring Pipes

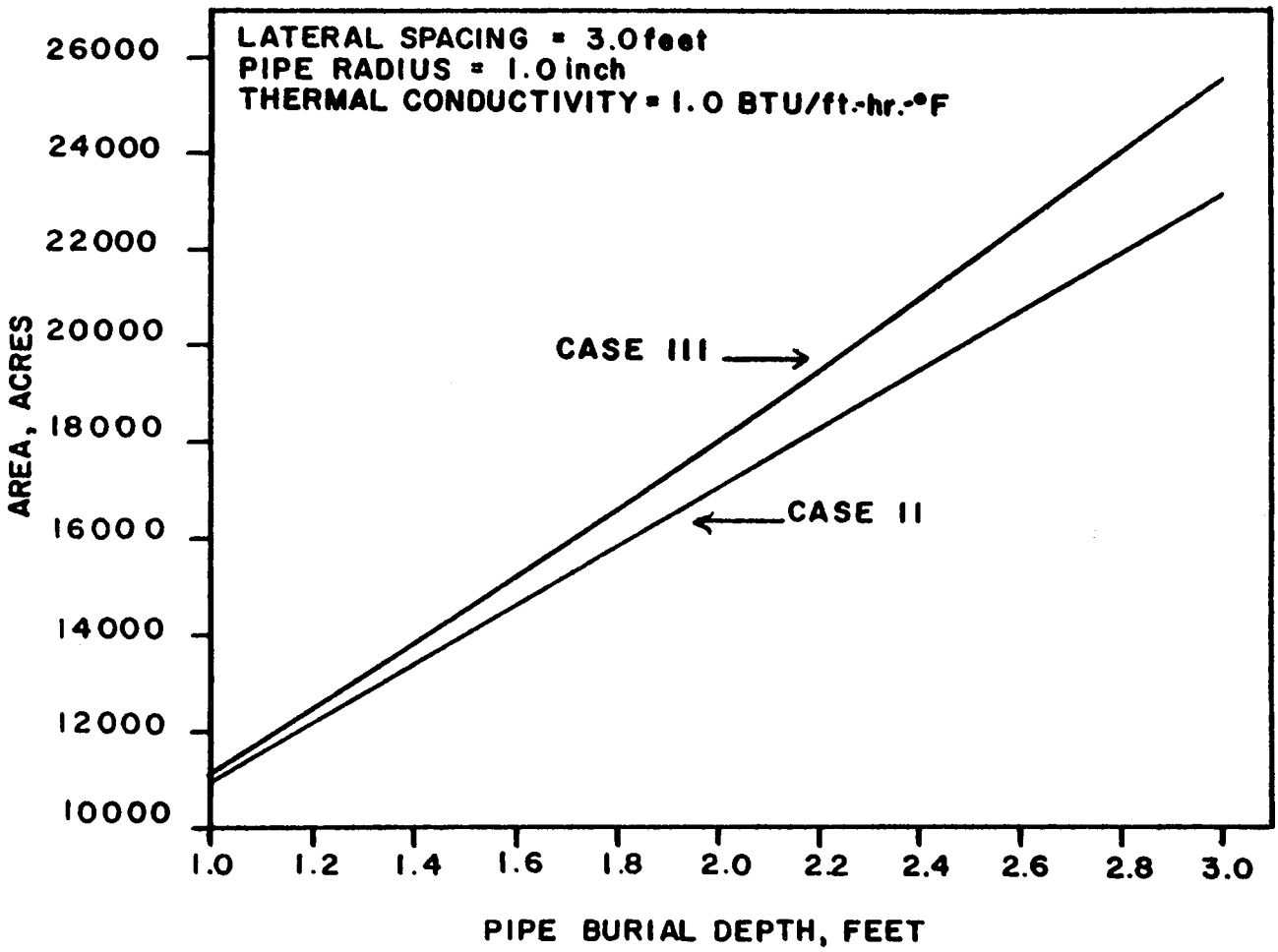

Figure 15 Effect Of Pipe Burial Depth On The Total Land Area Heated By Condenser Cooling Water From A 1000 Megawatt Nuclear-Powered Steam Generation Electric Power Plant Carried In Soil Warming Systems With Water Flowing In The Same Direction In Neighboring Pipes (CASE II) And With Water Flowing In Opposite Directions In Neighboring Pipes (CASE III)

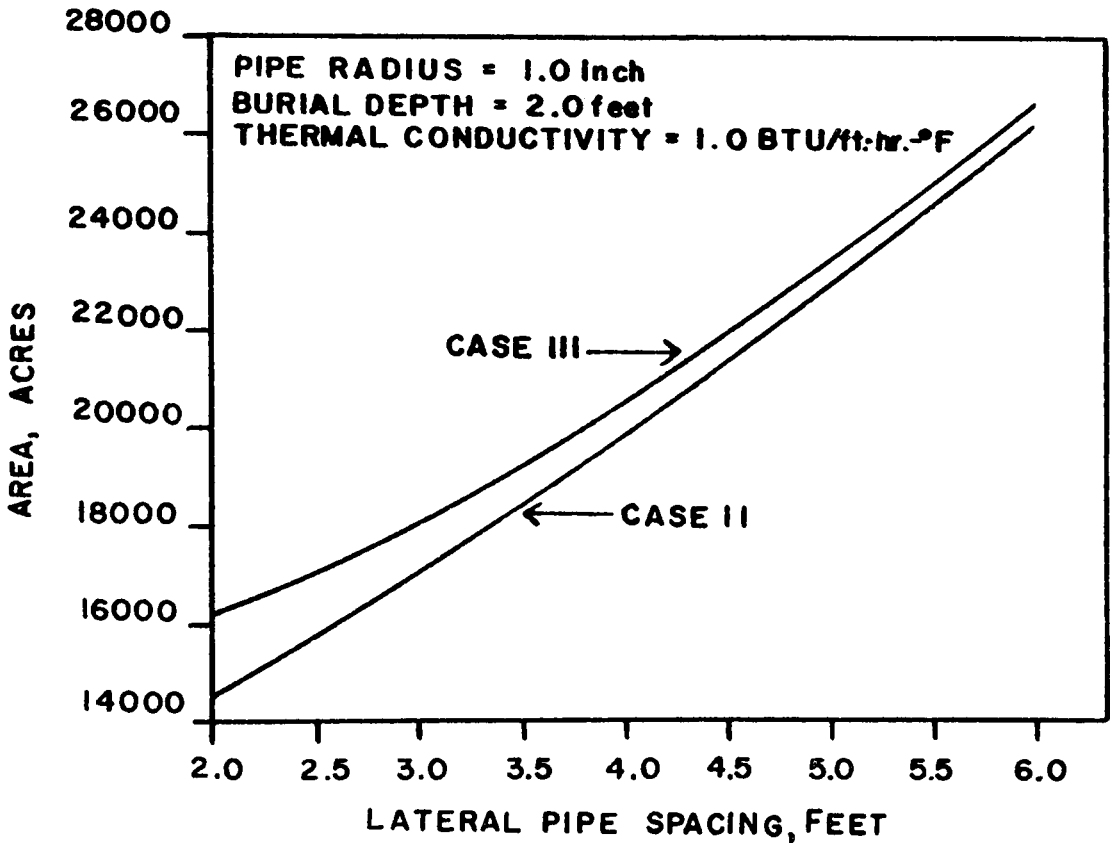

Figure 16 Effect Of Lateral Pipe Spacing On The Total Land Area Heated By Condenser Cooling Water From A 1000 Megawatt Nuclear-Powered Steam Generation Electric Power Plant Carried In Soil Warming Systems With Water Flowing In The Same Direction In Neighboring Pipes (CASE II) And With Water Flowing In Opposite Directions In Neighboring Pipes (CASE III)

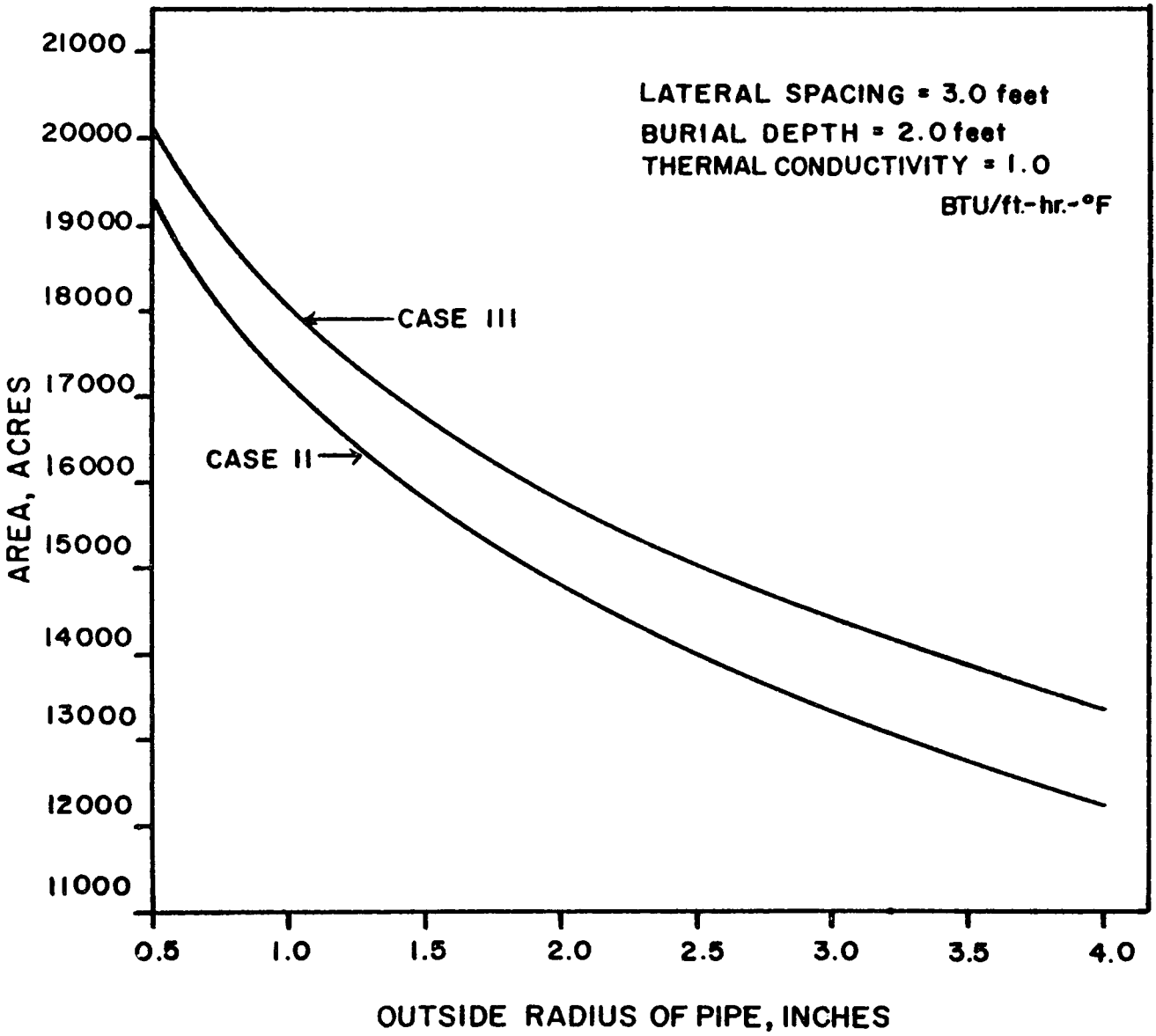

Figure 17 Effect Of Pipe Radius On The Total Land Area Heated By Condenser Cooling Water From A 1000 Megawatt Nuclear-Powered Steam Generation Electric Power Plant Carried In Soil Warming Systems With Water Flowing In The Same Direction In Neighboring Pipes (CASE II) And With Water Flowing In Opposite Directions In Neighboring Pipes (CASE III)

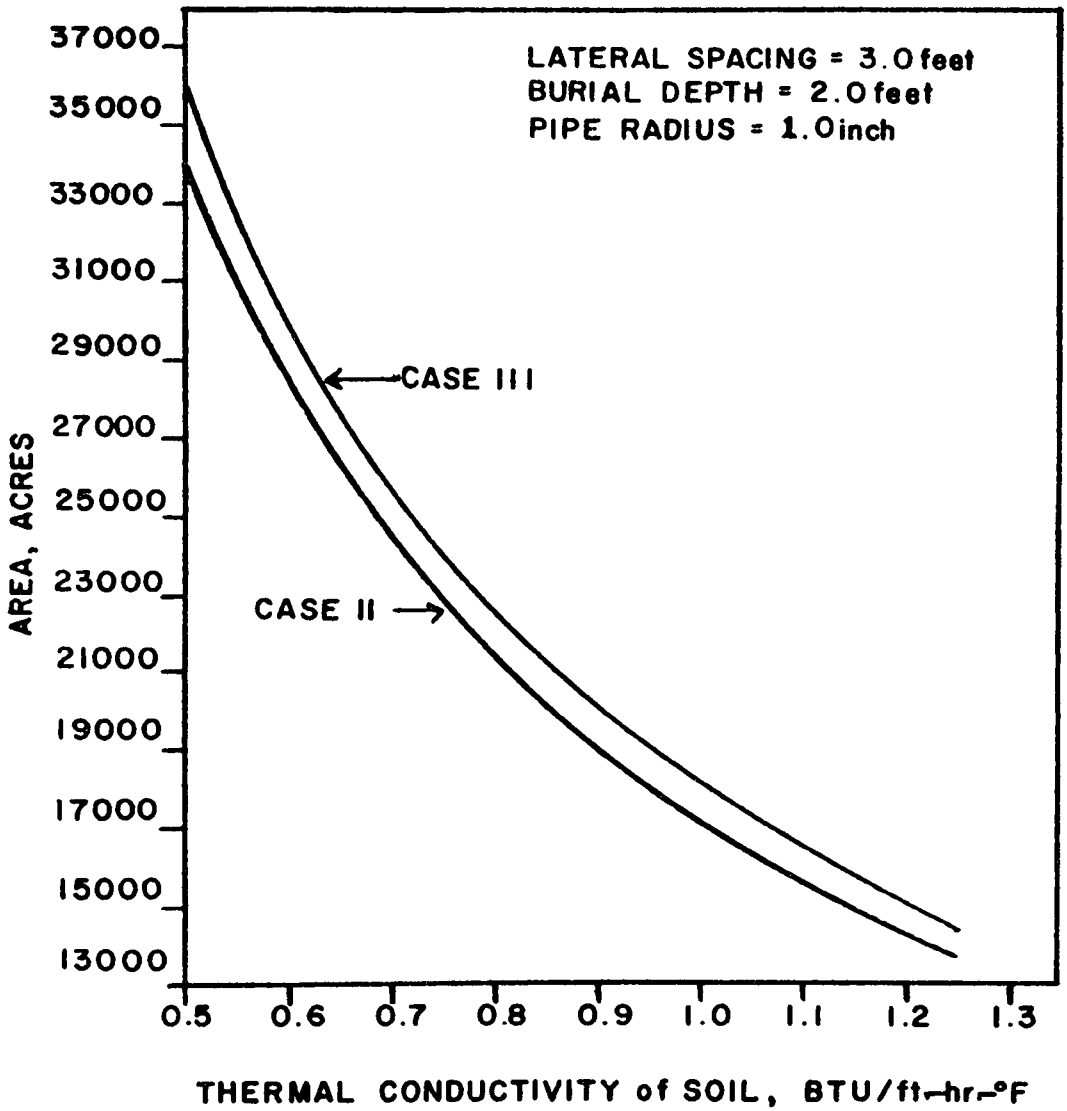

Figure 18 Effect Of Soil Thermal Conductivity On The Total Land Area Heated By Condenser Cooling Water From A 1000 Megawatt Nuclear-Powered Steam Generation Electric Power Plant Carried In Soil Warming Systems With Water Flowing In The Same Direction In Neighboring Pipes (CASE II) And With Water Flowing In Opposite Directions In Neighboring Pipes (CASE III)

V. DISCUSSION OF HEAT TRANSFER MODELS

The mathematical models developed here involve several assumptions which must be considered in their application. The assumptions have been made to simplify the problem suffiently to allow analytical solution. The important assumptions are:

1. Constant,uniform soil thermal conductivity.
2. No radial temperature variation in the water; pipe wall temperature equal to water temperature.
3. Constant, uniform soil surface temperature.
4. Steady-state operation.
5. The heat transfer in the soil is by conduction.
6. Heat is transferred in the soil in the radial direction only.

The assumption of constant, uniform thermal conductivity of the soil greatly simplifies the determination of the heat loss from a buried piping system. In design applications, a survey of the soil thermal conductivity should be conducted at the site of the proposed soil warming system. If the soil thermal conductivity does not vary greatly throughout the site, an average value of the thermal conductivity can be used in the mathematical models developed herein. If the soil thermal conductivity does vary significantly at the site, the proposed site can be divided, for purposes of analysis, into two or more "homogeneous" sections. The mathematical models then can be applied to each section.

For turbulent flow the assumption of no radial variation in the water temperature is reasonable. The thermal conductivity

of most pipe construction materials is large compared to the soil thermal conductivity; thus the resistance to heat flow through the wall of the pipe can be ignored. Under the conditions of turbulent flow and a pipe wall of high thermal conductivity, the water temperature is approximately equal to the outside pipe wall temperature.

In their present form, these mathematical models omit daily and seasonal soil temperature variations. The use of maximum soil surface temperature in the mathematical models will give conservative estimates of the land area required. It is possible to extend the proposed mathematical models to account for the seasonal temperature variation of the soil by assuming that the soil warming system responds instantly to a soil surface temperature change. However, the results of previous work on the response time of soil warming systems suggests that systems respond very slowly to such temperature changes. The time required for the proposed soil warming systems to reach steady-state operation is not considered in the models. The heat transferred from the pipe system will be minimum when the system is operating at steady state.

In addition to heat transfer in the soil by conduction, energy is transferred by moisture migration in both the liquid and vapor phases. The error resulting from omitting these modes of energy transfer will depend on the thermal conductivity and moisture content of the soil at the proposed site. Extension of the models to include effects of moisture movement may be necessary to allow practical usage in some cases.

The mathematical models developed here also assume heat transfer in the soil in the radial direction only. It has been determined experimentally that the temperature gradient in the radial direction is of the order of magnitude of 10^5 greater than the temperature gradient in the longitudinal direction. Therefore, omission of heat transfer in the longitudinal direction should not cause significant error.

As can be seen from Figures 15, 16, 17, and 18, the piping layout with opposite flow direction in neighboring pipes serves slightly more land area than the single flow direction arrangement, for equal amounts of heat dissipation. By comparing Figures 10, 11, 12, and 13 with Figures 5, 6, and 7, one sees that the opposite flow direction arrangement results in a more even temperature distribution throughout the field than is obtained with the single flow direction arrangement. This result is further exemplified by a comparison of Figures 14 and 8, which show the average temperature of the soil one foot below the surface of the ground versus longitudinal position for the two flow arrangements. An even soil temperature distribution in the root zone can be important if the crop to be grown in the field is sensitive to the temperature of the soil around its roots.

Figures 15, 16, 17, and 18 show the effects of various parameters on the total land area required to dissipate a given amount of heat. The most critical parameter is the soil thermal conductivity, which is a strong function of the moisture content of the soil. Water serves to fill

the voids in the soil, thus increasing the thermal conductivity of the soil by substituting water for air in the voids. Other investigators (19) have observed that soil moisture migrates away from a hot pipe, creating a dry core around the pipe. This dry core has a low thermal conductivity and reduces the heat disposal efficiency of the soil warming system. These facts emphasize the need to maintain a wet soil.

Figures 15 and 16 show the effect of lateral spacing and pipe burial depth on the total land area required to dissipate a given amount of heat. It appears that a closely spaced, shallowly buried system of pipes would yield the minimum land area required to dissipate a given amount of thermal energy. It must be stressed, however, that the mathematical models assume an isothermal soil surface. As the pipes are moved closer together and nearer the ground surface, this assumption becomes questionable. However, for most agricultural uses the pipes would have to be buried at least one foot deep to allow for cultivation, and therefore this assumption does not appear to impose major limitations on the use of the models.

VI. DEVELOPMENT OF MATHEMATICAL MODELS FOR SIMULTANEOUS HEAT AND MOISTURE TRANSFER

Consider the process of moisture flow through a non-uniform temperature soil section with the following simplifying assumptions (which the investigators believe to be defensible in many practical situations of interest and importance, including subsurface irrigation with warm water).

1. Assume the soil is not saturated with water, but that the moisture content is high enough that a continuous liquid phase is present.
2. Ignore the presence of dissolved salts in the water phase.
3. Assume that the flow of water through the soil in the vapor phase is negligible in comparison with the flow in the liquid phase. (The validity of this assumption will depend on the temperature of the water in the soil and on the moisture content of the soil).
4. Ignore adsorption forces between the liquid phase and solid soil particles.

Define a thermodynamic "system" for analysis by location of the boundary so as to include the liquid phase (water) only, excluding a surface layer of a few molecular thicknesses adjacent to any phase discontinuity (liquid-gas, liquid-solid). The system is then an open system, i.e., mass is transferred into and out of the system at the locations where the boundary of the soil section cuts across the liquid water phase. The system boundary specified will be very irregular, with a high area to volume ratio.

The system is single-component, liquid water, and the equation of change (local balance equation) which describes the variation of internal energy (total energy minus macroscopic kinetic and macroscopic potential energies) can be written as (20):

$$\frac{\partial \rho \bar{U}}{\partial t} = - \nabla \cdot \rho \bar{U} \vec{v} + \nabla \vec{v} : \vec{\vec{\sigma}} - \nabla \cdot \vec{J}_q \qquad (1)$$

where

ρ = local density

$\bar{U}$ = local internal energy per unit mass

$\vec{v}$ = local velocity (vector)

$\vec{\vec{\sigma}}$ = local, generalized stress tensor

$\vec{J}_q$ = local heat flow rate (vector)

t = time .

The left side of Equation (1) can be identified as the local rate of accumulation of internal energy. The terms on the right side are associated with mass transfer, work transfer, and heat transfer respectively.

Using the definition of the "substantial derivative" operator,

$$\frac{D}{Dt} = \frac{\partial}{\partial t} + \vec{v} \cdot \nabla \qquad (2)$$

One can rewrite Equation (1) as

$$\rho \frac{D\bar{U}}{Dt} = - \nabla \cdot \vec{J}_q + \nabla \vec{v} : \vec{\vec{\sigma}} \, . \qquad (3)$$

For a single-component system, with no surface effects (there is no surface tension at the boundary of the system), the fundamental property relation of thermodynamics (Gibbs Equation) can be written as

$$\frac{D\bar{U}}{Dt} = T \frac{D\bar{S}}{Dt} - P_E \frac{D\bar{V}}{Dt} \qquad (4)$$

where P_E is the external pressure on the system.

Now considering Equation (3), the internal energy balance equation, one must be able to describe the general stress tensor in terms of macroscopically observable properties. It is a basic assumption of fluid mechanics that the stress tensor in a fluid in motion can be decomposed into an "equilibrium" part and a "nonequilibrium" part as follows:

$$\vec{\vec{\sigma}} = - P_E \vec{\vec{I}} - \vec{\vec{\Pi}} \tag{5}$$

where

P_E = "equilibrium" pressure, equal to external pressure

$\vec{\vec{\Pi}}$ = component of stress tensor related to velocity gradients

$\vec{\vec{I}}$ = the unit tensor .

The writers contend that in the case where surface effects are not negligible the generalized stress tensor can be represented as

$$\vec{\vec{\sigma}} = -P_E \vec{\vec{I}} - \vec{\vec{\Pi}} - \vec{\vec{\Pi}}_s \tag{6}$$

where

$\vec{\vec{\Pi}}_s$ is a component of the stress tensor induced by surface tension effects. If one further assumes $\vec{\vec{\Pi}}_s$ to be isotropic, the relation can be rewritten as

$$\vec{\vec{\sigma}} = - (P_E + P_s) \vec{\vec{I}} - \vec{\vec{\Pi}} \tag{7}$$

where it has been assumed that

$$\vec{\vec{\Pi}}_s = P_s \vec{\vec{I}} .$$

Combining Equations (3), (4) and (7), and ignoring the stress tensor components associated with velocity gradients, one can write

$$\rho \frac{D\bar{S}}{Dt} = \frac{-\nabla \cdot \vec{J}_q}{T} - \frac{P_s \nabla \cdot \vec{v}}{T} . \tag{8}$$

Equation (8) can be rearranged to give

$$\frac{\partial \rho \bar{s}}{\partial t} = -\nabla \cdot \rho \vec{v} \bar{S} - \nabla \cdot \frac{\vec{J}_q}{T} - \frac{\vec{J}_q}{T^2} \cdot \nabla T - \nabla \cdot \frac{P_s \vec{v}}{T} + \vec{v} \cdot \nabla \frac{P_s}{T} . \tag{9}$$

Equation (9) is a local balance equation for entropy. Integration over the volume of the system, V(t), with area A(t), yields

$$\frac{d}{dt} \int_V \rho \bar{s} dV = - \int_A \left[\rho (\vec{v} - \vec{v}_b) \bar{s} + \frac{P_s \vec{v}}{T} \right] \cdot \vec{n} dA - \int_{A_s} \frac{\vec{J}_q}{T} \cdot \vec{n} dA$$

$$+ \int_V \left[- \frac{\vec{J}_q}{T^2} \cdot \nabla T + \vec{v} \cdot \frac{P_s}{T} \right] dV. \tag{10}$$

The integral terms on the R.H.S. of Equation (10) are, from left to right respectively,

1) the net rate of entropy transfer to the system associated with mass flow across the boundary,
2) the net rate of entropy transfer to the system associated with heat transfer across the boundary, and
3) the rate at which entropy is <u>produced</u> in the system.

The entropy production term consists of the sum of the product of "fluxes" and conjugate "forces." The two fluxes can be easily identified with macroscopically measurable quantities if the entropy production expression is written as follows:

$$\dot{S}_p = \vec{J}_q \cdot \nabla \frac{1}{T} + \frac{\vec{J}_w}{\rho} \cdot \nabla \frac{P_s}{T} \tag{11}$$

where

$\dot{S}_p$ = rate of entropy production

$\vec{J}_q$ = heat flux

$\vec{J}_w = \rho\vec{v}$, mass (moisture) flux

T = absolute temperature

P_s = internal "pressure" due to curvature of liquid surface.

Following the method of irreversible thermodynamics, assume a linear functional relationship between fluxes and forces as follows:

$$\vec{J}_q = L_{11} \nabla \frac{1}{T} + L_{12} \nabla (P_s/T)$$
$$\vec{J}_w = L_{21} \nabla \frac{1}{T} + L_{22} \nabla (P_{s/T}). \qquad (12)$$

Equation(s) (12) are local equations, i.e., apply at any point in the system specified. However, as was pointed out by Groenvelt and Bolt (21), experimental measurements of flow in porous systems are limited to fluxes integrated over a cross-section of the system. Equations (12) then should be integrated over a cross-section of soil perpendicular to the bulk, macroscopic flow direction. In this context, we stipulate that in Equations (12) the coefficients L_{11}, L_{12}, L_{21}, L_{22} are based on a unit cross-section of the soil-water-air system. L_{11} then can be related to the thermal conductivity of Fourier's Law, L_{22} is a phenomenological coefficient relating mass flow rate to pressure gradient in a fluid, and L_{12} and L_{21} are the so-called "cross-coefficients" relating heat and mass transfer to gradients in pressure and temperature respectively.

L_{11} can be estimated from thermal conductivity measurements on moist soil (as a function of moisture content). Recalling that P_s is the internal "pressure" component due to surface tension and surface curvature, and noting that the surface curvature depends directly on the moisture content for unsaturated soil, one can write

$$\nabla P_s = \frac{d}{dx} P_s = \frac{dP_s}{d\theta} \nabla\theta \tag{13}$$

where

θ = fractional moisture content = moisture content/ moisture content at saturation .

The value of P_s, which varies greatly from point to point, cannot be measured directly. However, the standard "soil tension" measurement is an integrated value of P_s (integrated over large enough volume that pressure variations are not evidenced except as the degree of saturation changes).

Furthermore,

$$\nabla(P_s/T) = \frac{\nabla P_s}{T} - P_s \frac{\nabla T}{T^2} \tag{14}$$

and, although gradients in pressure may be large because of the strong effect of θ on P_s, temperature gradients are much smaller (in the present application). Therefore assume

$$\nabla \frac{P_s}{T} \simeq \nabla P_s/T. \tag{15}$$

One then can rewrite Equations (12) as

$$\vec{J}_q = -\frac{L_{11}}{T} \nabla \ln T + L'_{12} \nabla\theta \tag{16-a}$$

$$\vec{J}_w = -\frac{L_{21}}{T} \nabla \ln T + L'_{22} \nabla\theta \tag{16-b}$$

where

$$L'_{12} = \frac{L_{12}}{T} \frac{dP_s}{d\theta}$$

$$L'_{22} = \frac{L_{22}}{T} \frac{dP_s}{d\theta} .$$

Estimates of L_{11} and L_{22} can be obtained from literature measurements of thermal conductivity and soil moisture diffusion.

Because as Cary and Taylor (12) have shown, Equations (16) hold for all values of the flux, including $\vec{J}_w = 0$, the ratio of L_{21} to L_{22} must be given by

$$\frac{L_{21}}{TL'_{22}} = \left[\frac{\nabla\theta}{\nabla \ln T} \right]_{\vec{J}_w = 0} = \beta^* \qquad (17)$$

and

$$\vec{J}_w = L'_{22} \left[-\beta^* \nabla \ln T + \nabla\theta \right] . \qquad (18)$$

Using Onsager's relation (2)

$$L_{12} = L_{21} = L'_{12} T \Big/ dP_{s/d\theta} = \beta^* T L'_{22} . \qquad (19)$$

Therefore one can write

$$\vec{J}_q = -\frac{L_{11}}{T} \nabla \ln T + \beta L'_{22} \nabla\theta \qquad (20)$$

where

$$\beta = \beta^* dP_{s/d\theta}.$$

The four phenomenological coefficients thus can be determined from experimental measurements. A summary of soil property data compiled during this study is included in Appendix II.

TEST OF MODEL WITH EXPERIMENTAL DATA

Gee (18) presented the experimental moisture content data shown in Table 1 for a sealed soil column operating at unsteady state

Table 1. Volumetric Moisture Content as a Function of Time and Distance From Warm End of a Sealed Soil Column With Combined Temperature and Moisture Content Gradients (From Gee [18])

Distance (cm)	Time (days)	Moisture Content	Distance (cm)	Time (days)	Moisture Content
1	0	0.150	5	0	0.152
	1	0.137		1	0.153
	4	0.085		4	0.159
	9	0.075		9	0.159
	14	0.065		14	0.166
	17	0.065		17	0.167
2	0	0.151	7	0	0.150
	1	0.154		1	0.150
	4	0.135		4	0.157
	9	0.086		9	0.183
	14	0.076		14	0.193
	17	0.074		17	0.193
3	0	0.150	9	0	0.150
	1	0.155		1	0.160
	4	0.154		4	0.198
	9	0.109		9	0.220
	14	0.090		14	0.227
	17	0.089		17	0.227
4	0	0.150			
	1	0.155			
	4	0.158			
	9	0.149			
	14	0.125			
	17	0.122			

with combined temperature and moisture gradients. Using Gee's steady state moisture and temperature profiles (for times greater than 14 days), the writers have calculated β^* and β by Equations (17) and (20). Values of $dP_s/d\theta$ were taken from matric suction vs. moisture content data presented by Gee (18). It should be noted that β^* and β vary markedly as a function of moisture content. Values of the soil moisture diffusivity, L'_{22}, also were taken from Gee (18). Using the data given in Table 1, the writers computed the instantaneous moisture flux $\vec{J}_w$ as a function of time and position in the column as follows.

The continuity equation can be written as

$$\frac{\partial \rho}{\partial t} = -\nabla \cdot \rho\vec{v} = -\nabla \cdot \vec{J}_w = -\frac{\partial \vec{J}_w}{\partial x} = \rho_s \frac{\partial \theta}{\partial t} \qquad (21)$$

where

$\vec{J}_w$ = moisture flux

ρ_s = soil-water-air system density, assumed constant.

It follows from Equation (21) that the flux of moisture must be computed from the following relation when the flow is unsteady - state;

$$\frac{\vec{J}_w}{\rho} = -\int_o^x \left[\frac{\partial \theta}{\partial x}\right]_x dx$$

where x = position (measured from the end) in the column.

The following steps were performed.

1. Plot θ vs. t as a function of x.
2. At a given x, determine, graphically, $d\theta/dt$ as a function of t.
3. Plot $d\theta/dt$ vs. x as a function of t.

4. Graphically integrate the plot of step 3 from 0 to x to obtain actual flow rate (flux) as a function of x and t.

The actual moisture flow rates so obtained are compared with predicted moisture flow rates computed by Equations(16) in columns 3, 4,and 5 of Table 2. The arithmetic mean of the ratios of observed to predicted moisture flow rates was 1.0054 with a standard deviation of 0.359. This agreement is considered as substantiating the model, for the range of moisture content shown, in view of the method of experimental determination of $\vec{J}_w$ which required extensive graphical analysis, and the expected experimental error. (Note that Gee concluded, incorrectly the writers believe, that his data showed the Cary and Taylor model to be invalid.)

VII. APPLICATION OF MATHEMATICAL MODELS FOR SIMULTANEOUS HEAT AND MOISTURE TRANSFER

After an extensive literature search (23), the writers found no reference to any mathematical solutions of Equations(16) for boundary conditions similar to those in subsurface irrigation. The writers also find that the "cross-effects" (for example, mass flux due to temperature gradients and heat flux due to pressure or moisture content gradient), commonly are neglected on the basis of the argument that the cross-coefficients are small in comparison with the thermal conductivity and moisture diffusivity. Such an argument is not valid in general because it is the product of the coefficient and the force which must be considered rather than the coefficient alone. The magnitude of the force cannot be estimated without solution of the equations.

Table 2. Experimental vs. Predicted Moisture Flow Rates In a Sealed Soil Column With Combined Temperature and Moisture Content Gradients (Experimental Data from Gee [18])

Distance From Warm End of Column (cm)	Time (days)	Actual Flux Density (cm/day)	Predicted Flux Density (cm/day)	Ratio (Actual/ Predicted)	Volumetric Moisture Content
1	1	0.0510	0.00317	-	0.137
	4	0.0160	-0.00078	-	0.085
	9	0.00285	-0.00026	-	0.075
	14	0.0	-	-	0.065
2	1	0.0652	0.05295	1.23	0.154
	4	0.0210	-0.00681	-	0.135
	9	0.0096	-0.00005	-	0.086
	14	0.0005	-0.00008	-	0.076
3	1	0.0600	0.06177	0.97	0.155
	4	0.0295	0.04249	0.70	0.154
	9	0.0221	0.00158	-	0.109
	14	0.0025	0.00069	-	0.090
4	1	0.0509	0.06177	0.82	0.155
	4	0.0387	0.06177	0.63	0.158
	9	0.0355	0.01682	2.11	0.149
	14	0.0065	0.00900	-	0.125
5	1	0.0416	0.05295	0.79	0.153
	4	0.0392	0.05148	0.76	0.159
	9	0.0089	0.03397	1.15	0.159
	14	0.0374	0.02306	0.59	0.166
7	1	0.0374	0.03883	0.98	0.150
	4	0.0315	0.05868	0.54	0.157
	9	0.02975	0.00528	5.63*	0.183
	14	0.0062	0.00528	-	0.193
9	1	0.0204	0.01133	1.8	0.160

*Omitted from Statistical Analysis

The writers studied Equations (16) for a set of physical boundary conditions similar to those expected with a subsurface irrigation system. Consider the boundary conditions shown for one-dimensional mass and heat transfer in soil (omitting gravity effects) shown in Figure 19.

The configuration shown in Figure 19 which describes a cylinder of soil "suspended in air," with one-dimensional fluxes, is not accurately descriptive of heat and moisture transfer from a pipe buried in the soil. However, it was chosen for study so that the effects of inclusion of "coupling effects" could be studied first without the additional difficulties of having to solve the differential equations in two dimensions.

Steady-state balances on energy and mass in the unsaturated area indicated in Figure 1 give

$$\nabla \cdot \vec{J}_q + \nabla \cdot h_w \vec{J}_w = 0 \qquad (22\text{-a})$$

$$\nabla \cdot \vec{J}_w = 0 \qquad (22\text{-b})$$

where

h_w = specific enthalpy of water.

Substituting the expressions for $\vec{J}_q$ and $\vec{J}_w$ from Equations (16) and integrating the resulting equations with respect to radial distance from the pipe, r, gives (after considerable manipulation),

$$\frac{d\theta}{dr} = \frac{-1/2\pi r\ (\vec{J}_{w1}) - \rho D\ \beta^*/T\ (dT/dr)}{\rho D} \qquad (23\text{-a})$$

$$\frac{dT}{dr} = \frac{(-T/2\pi r)\ \ (\vec{J}_{q1} + h_{w1}\ \vec{J}_{w1}) - (\beta + h_w)\ \vec{J}_{w1}}{(L_{11} - \rho D\ \beta^*\ \beta)} \qquad (23\text{-b})$$

where

$\vec{J}_{q1}$ = heat flux at $r = R_1$ (at the pipe)

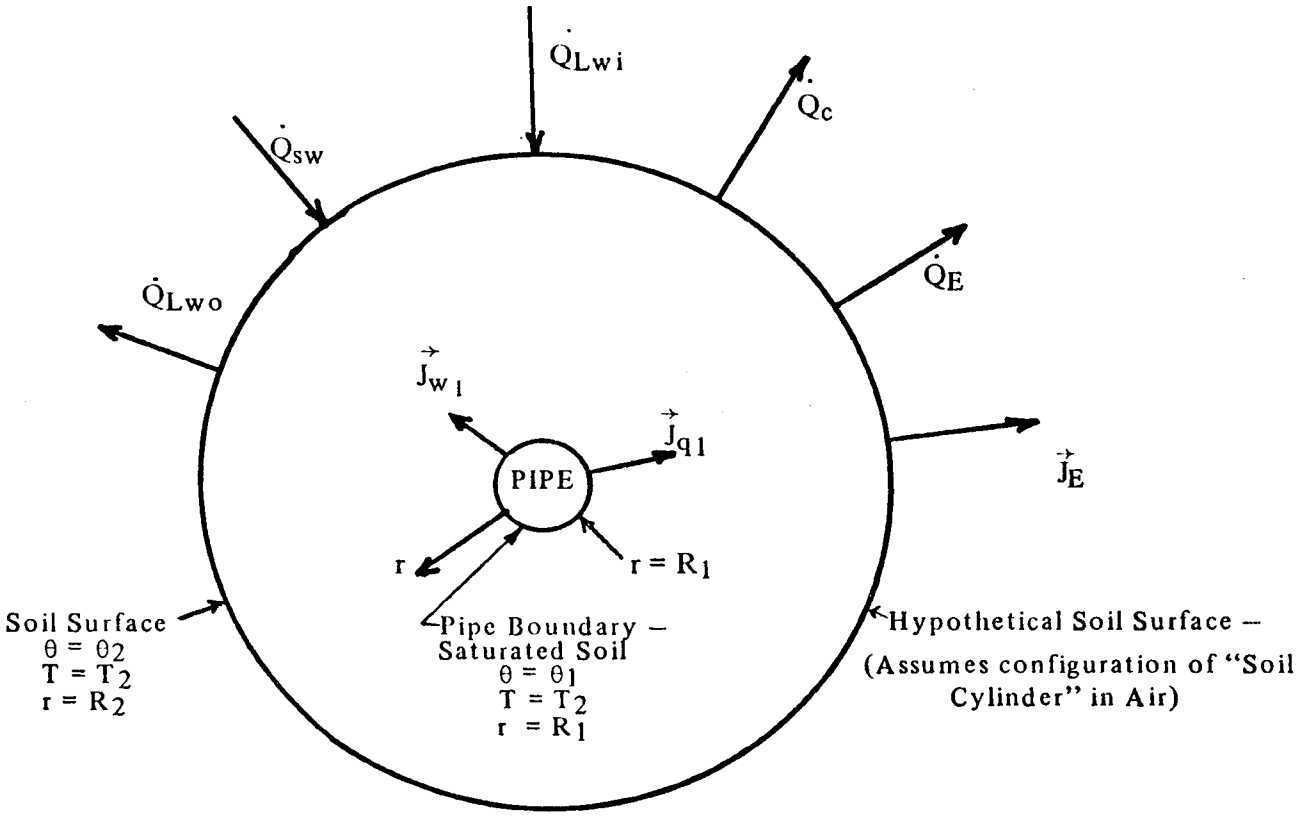

$\dot{Q}_{Lwo}$ = Long Wave Radiation from Soil Surface, cal/cm^2 – day

$\dot{Q}_{sw}$ = Short Wave Radiation to Soil Surface, cal/cm^2 – day

$\dot{Q}_{Lwi}$ = Long Wave Radiation to Soil Surface, cal/cm^2 – day

$\dot{Q}_c$ = Net Convective Heat Transfer, Soil to atmosphere, cal/cm^2 – day

$\dot{Q}_E$ = Energy Transfer, soil to atmosphere, with evaporation, cal/cm^2 – day

$\vec{J}_E$ = Evaporation mass flux, soil to atmosphere, gm/cm^2 – day

$\vec{J}_{w1}$ = Moisture Flux through soil at pipe, gm/cm^2 – day

$\vec{J}_{q1}$ = Heat Flux through soil at pipe, gm/cm^2 – day

Figure 19. Boundary Conditions For One-Dimensional Simulation of Subsurface Irrigation with Warm Water

$\vec{J}_{w_1}$ = moisture flux at r = R_1

h_{w_1} = specific enthalpy of water at r = R_1.

Equations (23) with the boundary conditions shown in Figure 1 constitute two simultaneous boundary value problems. One must find a value of $\vec{J}_{w_1}$ and $\vec{J}_{q1}$, by trial and error, which will satisfy the differential equations and the boundary conditions.

Equations (23) have four possible types of boundary conditions:

I. @ r = R_1, T = T_1, $\theta = \theta_1$

@ r = R_2, T = T_2, $\theta = \theta_2$

II. @ r = R_1, T = T_1, $\theta = \theta_1$

@ r = R_2, T = T_2, $\vec{J}_{w_2} = \vec{J}_{w_1} (R_1/R_2)$ (24)

III. @ r = R_1, T = T_1, $\theta = \theta_1$

@ r = R_2, $\vec{J}_{q_2} = \vec{J}_{q_1} (R_1/R_2)$, $\theta = \theta_2$

IV. @ r = R_1, T = T_1, $\theta = \theta_1$

@ r = R_2, $\vec{J}_{q_2} = \vec{J}_{q_1} (R_1/R_2)$, $\vec{J}_{w_2} = \vec{J}_{w_1} (R_1/R_2)$.

An actual soil surface undergoes almost constant changes in temperature and volumetric moisture content because of variations of climatic conditions, the season, the time of day, rainfall, evaporation, etc. If the temperature and volumetric moisture content of the soil surface are controlled by these "external" conditions but not by the heat and moisture transfer initiated by the source, Type I boundary conditions may be justified. Boersma [19, 24] observed for a field heated by buried electric cables that the temperature of the soil

surface was not increased by the cables, but for lower soil surface temperatures the heat transfer from the cables increased. Trezak and Obeng (25) showed that for lower soil surface temperature, the heat transfer from a buried source increased, but for a hundred-fold change in the convective heat transfer coefficient at the soil surface, no appreciable change occurred in the heat transfer from a buried source. These studies indicate that the heat transfer from a buried source is a function of the soil surface temperature but the soil surface temperature is not a strong function of the heat transfer from the buried source.

Type IV boundary conditions require specification of heat and mass flux at the soil-air interface. A steady-state energy balance on the soil gives

$$\vec{J}_{q_1} = \frac{R_2}{R_1} [\dot{Q}_C + \dot{Q}_E - \dot{Q}_{SW} - \dot{Q}_{LWi} + \dot{Q}_{LWo}]. \quad (25)$$

A steady-state mass balance gives:

$$\vec{J}_{w_1} = \frac{R_2}{R_1} [\vec{J}_E]. \quad (26)$$

Expressions for the various components of heat and mass flux from the surface can be written as functions of the soil surface properties, air properties, and the radiative heat flux in the atmosphere (23). Table 3 gives a summary of the relations used in this study. Literature sources are given in Bondurant's thesis (23). Equations (23) with both Type I and Type IV boundary conditions were integrated by means of the IBM Continuous Systems Modeling Program. The solutions required a lengthy trial and error search for the unknown

$$\dot{Q}_c = 86400\ (H)\ (W/4.47)\ (T_a - T_s)$$

where $\dot{Q}_c$ = convective heat transfer, cal/cm^2 – day
H = convective heat transfer coefficient, computed for a wind velocity of 2 meters/sec., 3.91×10^{-4} cal/cm^2 – sec – C
T_a = air temperature, C
T_s = soil surface temperature, C

$$\dot{Q}_{Lwi} = \beta_{ccf}\ (4.11 \times 10^{-8})\ [\ (T_a)\ (1.8)\ ]^4 \left[\frac{252}{(30.48)^2}\right]$$

where $\dot{Q}_{Lwi}$ = Long wave radiative heat transfer from air to soil surface, cal/cm^2 – day
β_{ccf} = cloud cover factor, usually taken as 0.8, dimensionless

$$\dot{Q}_{Lwo} = \varepsilon\ (4.11 \times 10^{-8})\ [\ (T_s)\ (1.8)\ ]^4 \left[\frac{252}{(30.48)^2}\right]$$

where $\dot{Q}_{Lwo}$ = Long wave radiation heat transfer from soil surface to air, cal/cm^2 – day
ε = emissivity of soil surface assumed equal to 0.8, dimensionless

$\dot{Q}_{sw}$ = 2280 cal/cm^2 – day (representative of ground level solar influx at mid-day in summer)

$$\dot{Q}_e = [\ \vec{J}_e / E_{sat}\ ]\ \dot{Q}_{vap}$$

where $\vec{J}_e$ = evaporation rate from soil surface, gm/cm^2 – day
E_{sat} = evaporation rate from saturated soil surface, gm/cm^2 – day
$\dot{Q}_{vap}$ = evaporation heat transfer from water surface, cal/cm^2 – day

and $\dot{Q}_{vap} = 11\ w\ [\ \mathrm{Exp}\ (21.6 - (5431.3/T_s)) - RH \cdot \mathrm{EXP}\ (21.6 - (5431.3)/T_a)\ )] \cdot [\ 252/(30.48)^2\ ]$

where w = wind velocity, mph
RH = relative humidity, dimensionless

$$\vec{J}_e = E_{sat}\ (\theta/\theta_{sat})^{\gamma}$$

where θ = soil moisture content
θ_{sat} = soil moisture content at saturation
γ = arbitrary coefficient, assumed equal to 1.0 for this study

$$E_{sat} = CH\ (\rho_{os} - \rho_{as})\ (86400)$$

where $C = 2.93 \times 10^{-3}$ gm – C/cm^2 – cal – mm Hg
ρ_{os} = saturated vapor pressure of soil surface, mm Hg
ρ_{as} = saturated vapor pressure of air, mm Hg

TABLE 3. SPECIFICATION OF BOUNDARY CONDITIONS

initial boundary condition. The primary difficulty apparently was due to the extreme mathematical "stiffness" of the differential equations (26). "Stiffness" refers to the requirement for extremely small integration step sizes to maintain numerical stability. Because of the extreme dependence of the moisture flow phenomenological coefficients on moisture content, the moisture profile may be very steep in some locations. In addition to the effect on stability, this behavior results in difficulties in the boundary value search for the second initial condition (heat and moisture flux at the inside boundary). Figure 20 shows this behavior, as it appears that a value of moisture flux of 16.3055 cm^3/cm day would result in the moisture content curve agreeing with the outside boundary condition. The extreme sensitivity of the solution to small changes in the inside moisture flux specification made the boundary value search very difficult. The results shown in Figure 20 were obtained only after a long series of runs in which the effects of different initial moisture and heat fluxes were studied.

Although we were not able to explore this numerical problem to a really satisfactory solution because of time limitations, the writers are continuing work on the computer solution of this type of model.

To compare the predicted results from Equations (23) with a similar model which omitted coupling effects, it was assumed that

$$\vec{J}_q = -\frac{L_{11}}{T} \nabla \ln T \tag{27}$$

$$\vec{J}_w = L_{22}' \nabla \theta$$

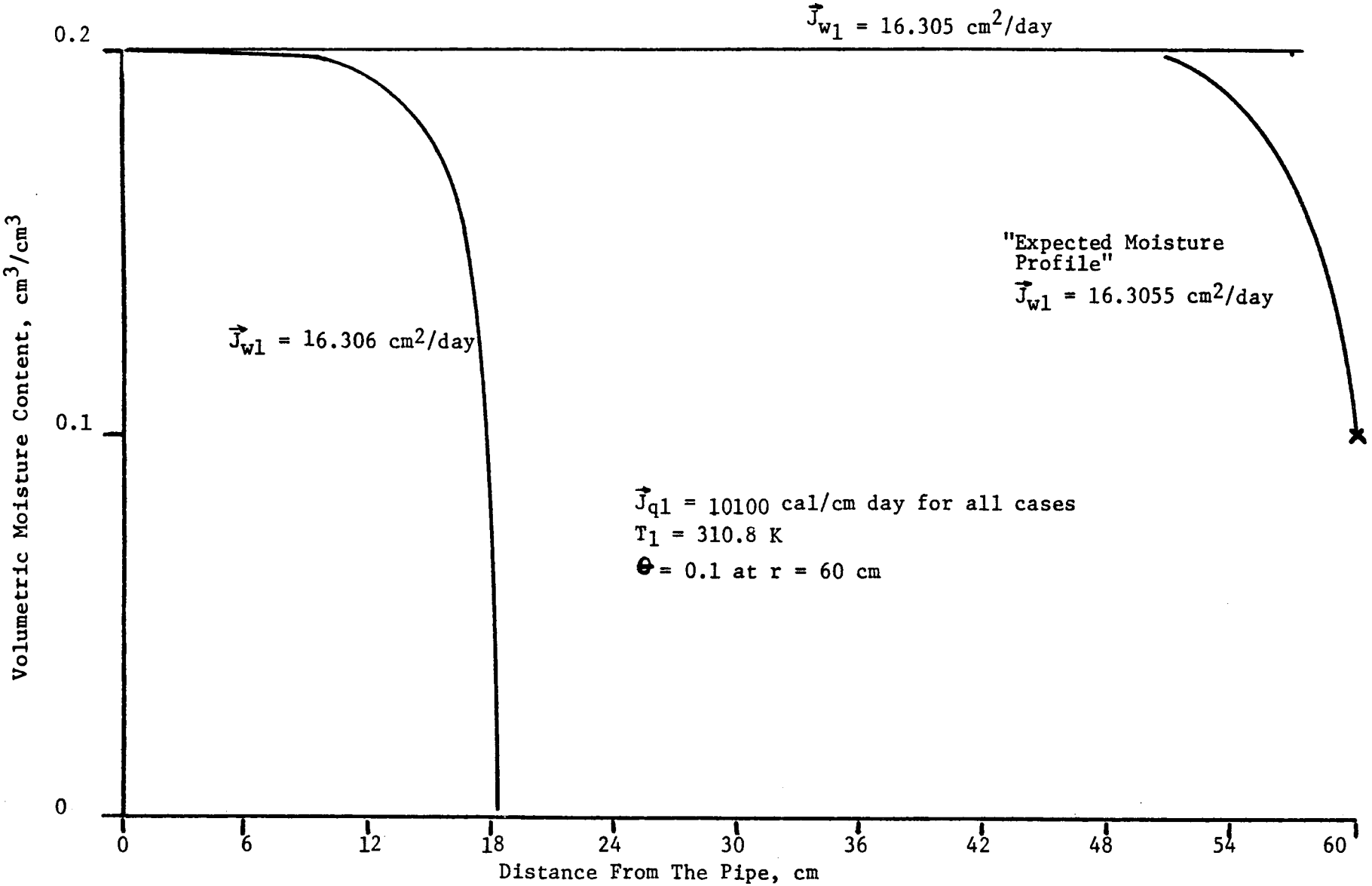

Figure 20. Volumetric Moisture Content vs. Distance From The Pipe

instead of

$$\vec{J}_q = -\frac{L_{11}}{T} \nabla \ln T + L'_{12} \nabla \theta \qquad (28)$$

$$\vec{J}_w = -\frac{L_{21}}{T} \nabla \ln T + L'_{22} \nabla \theta.$$

The model using Equations (27) did incorporate the effect of moisture content on thermal conductivity and therefore should provide for a valid comparison of the solutions to determine the effect of the "coupling" terms.

The result of a solution of the model using Equations 27, with other conditions the same as those specified for Figure 20, are shown in Figure 21. Comparison of Figures 20 and 21 indicates that the effect of coupling of heat and mass transfer on the prediction of heat transfer is small. However, because the predicted mass transfer is nearly thirty times greater with "coupling," it appears that the effect of coupling must be included in the model to predict moisture transfer accurately.

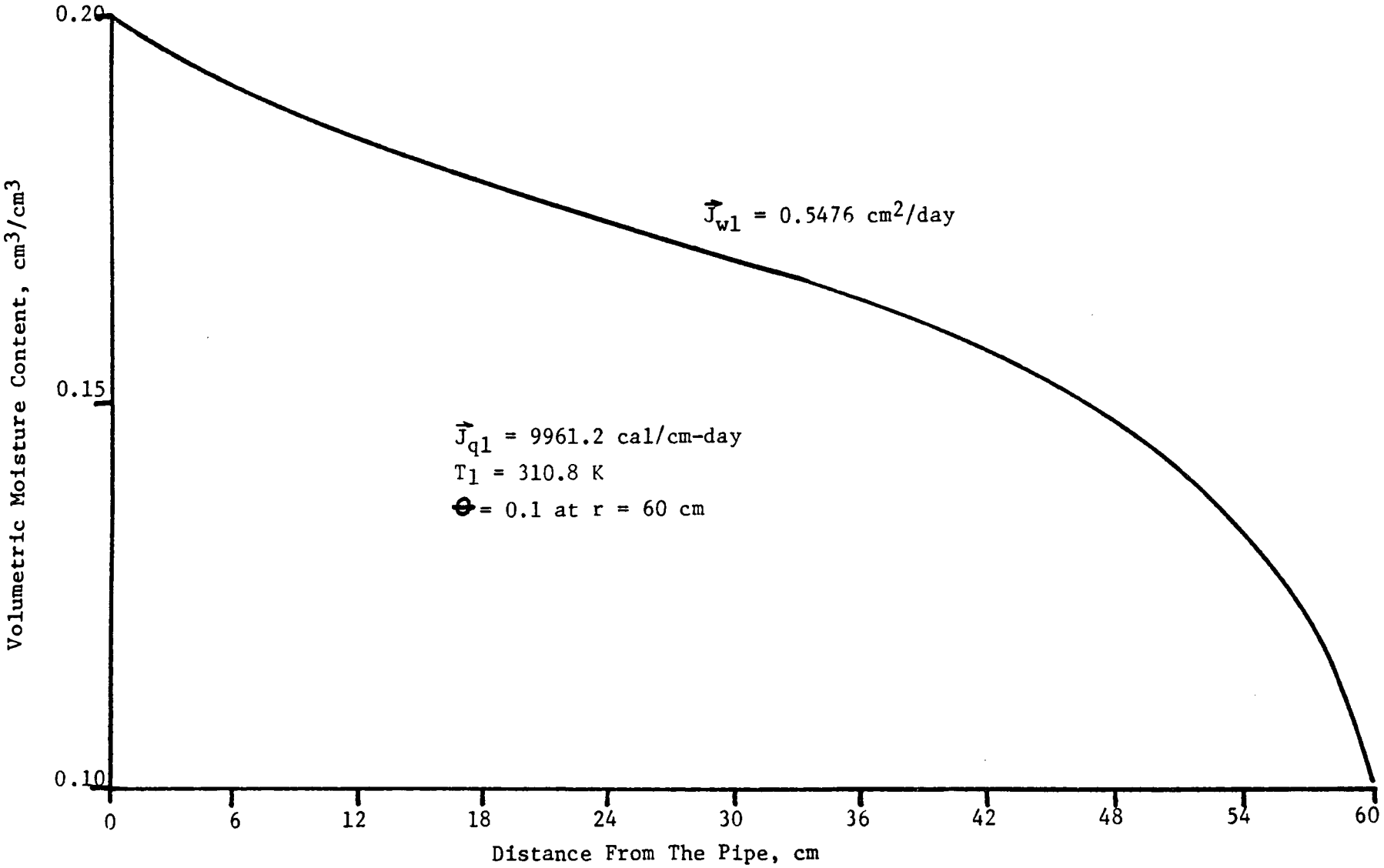

Figure 21. Volumetric Moisture Content vs. Distance From The Pipe, Simultaneous Heat and Moisture Transfer (Not Coupled)

VIII. Literature Cited

1. Parker, Frank L., and Peter A. Krenkel, Physical and Engineering Aspects of Thermal Pollution, CRC Press, Cleveland, Ohio (1970).

2. Boersma, L., "Beneficial Use of Waste Heat in Agriculture," 5th Annual Water Resources Research Conference, Washington, D.C., February 3, 1970.

3. Allen, John R., "Theory of Heat Losses from Pipes Buried in the Ground," American Society of Heating and Ventilation Engineers Journal, 26: 455 (1920).

4. Karge, Fritz, "Design of Oil Pipe Lines," The Petroleum Engineer, May, 1945, pp.76-78.

5. Kemler, Emory N., and Sabert Oglesby, Jr., Heat Pump Applications, McGraw-Hill, New York (1950).

6. Andrews, Robert V., "Solving Conductive Heat Transfer Problems with Electrical-Analogue Shape Factors," Chemical Engineering Progress, 51, 67 (1955).

7. Carslaw, H.S., Mathematical Theory of the Conduction of Heat in Solids, MacMillan and Co., Ltd., London (1921).

8. Jakob, Max, Heat Transfer: Vol. I, John Wiley & Sons, Inc., New York (1949).

9. Kutateladze, Samson Semenovich, Fundamentals of Heat Transfer, Academic Press Inc., New York (1963).

10. Schmill, J.V., "Variable Soil Thermal Resistivity--Steady State Analysis," IEEE Transactions on Power Apparatus and Systems, PAS-86, 215 (1967).

11. Philip, J.R., and D. A. DeVries, "Moisture Movement in Porous Materials Under Temperature Gradients", Transactions, American Geophysical Union, 38 (2): 222-232 (1957).

12. Cary, J. W., and S. A. Taylor, "Linear Equations for the Simultaneous Flow of Matter and Energy in a Continuous Soil System," Soil Science Society of America Proceedings, 28: 167-172 (1964).

13. DeGroot, S. R., and P. Mazur, Non-Equilibrium Thermodynamics, North Holland Publishing Company, Amsterdam (1962).

14. Fitts, D. D., Nonequilibrium Thermodynamics, McGraw-Hill, New York (1962).

15. Dirksen, C., and R. D. Miller, "Closed System Freezing of Unsaturated Soil," Soil Science Society of America Proceedings, 30: 168-173 (1966).

16. Fritton, D. D., D. Kirkham, and R. H. Shaw, "Soil Water Evaporation, Isothermal Diffusion, and Heat and Water Transfer," Soil Science Society of America Proceedings, 34: 183-189 (1970).

17. Cassel, D. K., D. R. Nielsen, and J. W. Biggar, "Soil Water Movement in Response to Imposed Temperature Gradients," Soil Science Society of America Proceedings, 33: 493-500 (1969).

18. Gee, G. W., Water Movement in Soils as Influenced by Temperature Gradients, Ph.D. Dissertation, Washington State University, Pullman (1966).

19. Boersma, L., "Warm Water Utilization," Proceedings of the Conference on the Beneficial Uses of Thermal Discharges, Albany, New York, New York State Dept. of Environmental Conservation, Albany, New York: 74-107 (1970).

20. Sliepcevich, C. M., K. Starling, and J. Havens, Thermodynamics of Continuous Systems, Air Force Office of Scientific Research Rpt. 563-66, Aug. 69.

21. Groenvelt, P. H., and G. H. Bolt, "Non-Equilibrium Thermodynamics of the Soil-Water System," Journal of Hydrology, 7:358-388 (1969).

22. Onsager, Lars, Physical Reviews, 37: 405 (1931) and 38: 2265 (1931).

23. Bondurant, John L., Coupled Heat and Moisture Transfer in Soil with Applications to the Design of a Warmwater Subsurface Irrigation System, M.S.Ch.E. Thesis, University of Arkansas, 1975.

24. Boersma, L., "Experimental Analysis of a Subsurface Soil Warming and Irrigation System Utilizing Waste Heat," personal communication, September 17, 1973.

25. Trezak, G. J. and D. Obeng, "An Analytical Consideration of Undersoil Heating," Journal of Environmental Quality, 2 (4): 458-462 (1973).

26. Curtiss, C. F., and Hirschfelder, J. O., "Integration of Stiff Equations," Proc. Natl. Acad. Sci., 38: 235 (1952).

27. Wilde, D. J., Optimum Seeking Methods, Prentice-Hall, Englewood Cliffs, New Jersey (1964).

28. Jackson, R. D., D. A. Rose, and H. L. Penman, "Circulation of Water in Soil Under a Temperature Gradient," Nature, 205: 314-316 (1965).

29. Philip, J. R., "Evaporation, Moisture and Heat Fields in the Soil," Journal of Meterology, 14:354-366 (1957).

30. Gardner, W. R., and M. S. Mayhugh, "Solutions and Tests of the Diffusion Equation for the Movement of Water in Soil," Soil Science Society of America Proceedings, 22: 197-201 (1958).

31. DeVries, D. A., Simultaneous Transfer of Heat and Moisture in Porous Media," Transactions, American Geophysical Union, 39(5): 909-916 (1958).

32. Gardner, W. R., "Diffusivity of Soil Water During Sorption as Affected by Temperature," Soil Science Society of America Proceedings, 23: 406-407 (1959).

33. Hanks, R. J., and S. A. Bowers, "Influence of Variations in the Diffusivity-Water Content Relation on Infiltration," Soil Science Society of America Proceedings, 27:263-265 (1963).

34. Hanks, R. J., and H. R. Gardner, "Influence of Different Diffusivity-Water Content Relations on Evaporation of Water From Soils," Soil Science Society of America Proceedings, 29:495-498 (1965).

35. Rose, C. W., "Water Transport in Soil with a Daily Temperature Wave, I: Theory and Experiment," Australian Journal of Soil Research, 6: 31-44 (1968).

36. Klute, A., "A Numerical Method for Solving the Flow Equation for Water in Unsaturated Materials," Soil Science, 73: 105-116 (1952).

37. Singh, R., and J. B. Franzini, "Unsteady Flow in Unsaturated Soils from a Cylindrical Source of Finite Radius,"Journal of Geophysical Research, 72(4): 1207-1215 (1967).

38. Neilsen, R. D., D. Kirkham, and W. R. van Wijk, "Diffusion Equation Calculations of Field Soil Water Infiltration Profiles," Soil Science Society of America Proceedings, 25 (3): 165-168 (1961).

39. Boersma, L., et al., Soil Water, American Society of Agronomy, Soil Science Society of America, Madison, Wisconsin (1972).

40. Gurr, C. G., T. J. Marshall, and J. T. Hutton, "Movement of Water in Soil due to a Temperature Gradient," Soil Science, 74 (5): 335-349 (1952).

41. Moore, R. E., "Water Conduction from Shallow Water Tables," Hilgardia, 12 (6): 383-426 (1939).

42. Hiler, E. A., and S. I. Bhuiyan, Dynamic Simulation of Unsteady Flow of Water in Unsaturated Soils and Its Application to Subirrigation Design, Water Resources Research Institute of Texas Agricultural and Mechanical University, Report No. 40 (1970).

43. Wang, F. C., and V. Lakshminarayana, "Mathematical Simulation of Water Movement Through Unsaturated Nonhomogeneous Soils," Soil Science Society of America Proceedings, 32: 329-334 (1968).

44. Wang, F. C., N. A. Hassan, and J. B. Franzini, "A Method of Analyzing Unsteady, Unsaturated Flow in Soils," Journal of Geophysical Research, 69: 2569-2577 (1964).

45. Klute, A., "Some Theoretical Aspects of the Flow of Water in Unsaturated Soils," Soil Science Society of America Proceedings, 16: 144-148 (1952).

46. Wilkinson, G. E., and A. Klute, "The Temperature Effect on the Equilibrium Status of Water Held by Porous Media," Soil Science Society of America Proceedings, 26: 326-329 (1962).

47. Moore, R. E., "The Relation of Soil Temperature to Soil Moisture, Pressure, Potential, Retention, and Infiltration Rate," Soil Science Society of America Proceedings, 5: 61-64 (1940).

Appendix I

SUPPLEMENTAL BIBLIOGRAPHY

1. Abd-El-Aziz, M. H., and S. A. Taylor, "Simultaneous Flow of Water and Salt through Unsaturated Porous Media," Soil Science Society of America Proceedings, 29(2):141-143 (1965).

2. Anderson, D. M., and A. Linville, "Temperature Fluctuations at a Wetting Front: I. Characteristic Temperature Time Curves," Soil Science Society of America Proceedings, 26:14-18 (1961).

3. Bearman, R. J., and J. G. Kirkwood, "Statistical Mechanics of Transport Processes: XI. Equations of Transport in Multi-component Systems," Journal of Chemical Physics, 28(1):136-145 (1951).

4. Biggar, J. W., and S. A. Taylor, "Some Aspects of the Kinetics of Moisture Flow into Unsaturated Soils," Soil Science Society of America Proceedings, 24:81-85 (1960).

5. Bird, R. B., W. E. Stewart, and E. N. Lightfoot, Transport Phenomena, John Wiley and Sons, New York (1960).

6. Bolt, C. H., and M. J. Frissel, "Thermodynamics of Soil Moisture," Netherlands Journal of Agricultural Science, 8:57-58 (1960).

7. Bouwer, H., "Theoretical Aspects of Unsaturated Flow in Drainage and Subirrigation," Agricultural Engineering, 40:395-400 (1959).

8. Bouyoucos, G. J., "The Effect of Temperature on Some of the Most Important Physical Processes in Soils," Michigan Agricultural Experiment Station, Technical Bulletin No. 22, 63 p. (1915).

9. Bryan, B. B., and G. Baker, "Small Diameter Plastic Pipe for Use in Subirrigation," Arkansas Farm Research, 8(6):7 (1964).

10. Buckingham, E., "Studies of the Movement of Soil Moisture," United States Department of Agriculture, Bureau of Soils, Bulletin No. 38, 61 p. (1907).

11. Cary, J. W., "An Evaporation Experiment and its Irreversible Thermodynamics," Internation Journal of Heat and Mass Transfer, 7:531-538 (1964).

12. Cary, J. W., "Onsager's Relation and the Non-Isothermal Diffusion of Water Vapor," Journal of Physical Chemistry, 67:126-129 (1968).

13. Cary, J. W., "Soil Moisture Transport Due to Thermal Gradients: Practical Aspects," Soil Science Society of America Proceedings, 30:428-433 (1966).

14. Cary, J. W., "Water Flux in Moist Soil: Thermal vs. Suction Gradients," Soil Science, 100(3):168-175 (1965).

15. Cary, J. W., R. A. Kohl, and S. A. Taylor, "Water Adsorption by Dry Soil and Its Thermodynamic Functions," Soil Science Society of America Proceedings, 28:309-314 (1964).

16. Cary, J. W. and H. F. Mayland, "Salt and Water Movement in Unsaturated Frozen Soil," Soil Science Society of America Proceedings, 36:539-543 (1972).

17. Cary, J. W., and S. A. Taylor, "The Dynamics of Soil Water: II. Temperature and Solute Effects," In: Irrigation of Agricultural Lands, R. M. Hagan, H. R. Haise, and T. W. Edminster, editors, American Society of Agronomy, Monograph No. 11, Madison, Wisconsin (1967).

18. Cary, J. W., and S. A. Taylor, "The Interaction of the Simultaneous Diffusion of Heat and Water Vapor," Soil Science Society of America Proceedings, 26:413-416 (1962).

19. Cary, J. W., and S. A. Taylor, "Thermally Driven and Vapor Phase Transfer of Water and Energy in Soil," Soil Science Society of America Proceedings, 26:417-420 (1962).

20. Clinton, F. M., "Invisible Irrigation of Egin Bench," Reclamation Era, 34(10): 192-184 (1948).

21. Davidson, B., and R. W. Bradshaw, "Thermal Pollution of Water Systems," Environmental Science and Technology, 1(8):618-630.

22. Denbigh, K. G., The Thermodynamics of the Steady State, Methuen and Co., LTD, London (1951).

23. Deryaguen, B. V., and M. K. Melnikova, "Experimental Study of the Migration of Water Through the Soil Under the Influence of Salt Concentration, Temperature, and Moisture Gradients," International Congress of Soil Science, 6th:305-314, Paris, France (1956).

24. Deryaguen, B. V., and M. R. Melinkova, "Mechanism of Moisture Equilibrium and Migration in Soils," In: Water and Its Conduction in Soils, Highway Research Board, Commission on Physico-Chemical Phenomena in Soils, Special Report No. 40, 43-54 (1959).

25. DeVries, D. A., "Some Remarks on Gaseous Diffusion in Soils," Transactions, International Congress of Soil Science, 4th (2): 41-43 (1950).

26. DeVries, D. A., "Some Remarks on Heat Transfer by Vapour Movement in Soils," Transactions, International Congress of Soil Science, 4th, (2): 38-41 (1950).

27. DeWiest, R. M., editor, Flow Through Porous Media, Academic Press, New York (1969).

28. Edlefsen, N. E., and A. B. C. Anderson, "The Thermodynamics of Soil Moisture," Hilgardia, 15:31-299 (1943).

29. Ferguson, H., P. L. Brown, and D. D. Dickey, "Water Movement Under Frozen Soil Conditions," Soil Science Society of America Proceedings, 28:700-203 (1964).

30. Fox, R. L., J. T. Phelan, and W. D. Criddle, "Design of Subirrigation Systems," Agricultural Engineering, 37:103-108 (1956).

31. Gardner, W. R., "Mathematics of Isothermal Water Conduction in Unsaturated Soils," In: Water and Its Conduction in Soils, Highway Research Board, Commission on Physico-Chemical Phenomena in Soils, Special Report No. 40, 78-87 (1958).

32. Globus, A. M., "Mechanisms of Soil and Ground Moisture Migration and of Water Movement in Freezing Soils Under the Effect of Thermal Gradients," Soviet Soil Science, 2:130-139 (1962).

33. Hadas, A., "Simultaneous Flow of Water and Heat Under Periodic Heat Fluctuations," Soil Science Society of America Proceedings, 32:297-301 (1968).

34. Harmathy, T. Z., Simultaneous Moisture and Heat Transfer in Porous Systems with Particular Reference to Drying, Industrial and Engineering Chemistry Fundamentals, 8(1):92-103 (1969).

35. Henry, P. S. H., "Diffusion in Absorbing Media," Proceedings, Royal Society of London, 171A:215-241 (1939).

36. Henry, P. S. H., "The Diffusion of Moisture and Heat Through Textiles," Discussions of the Faraday Society, 3:243-257 (1958).

37. Hillel, D., Soil and Water, Physical Principles and Processes, Academic Press, New York (1971).

38. Hougen, O. A., K. M. Watson, and R. A. Ragatz, Chemical Process Principals, II: Thermodynamics, John Wiley and Sons, New York (1966).

39. Hubbert, M. K., "Darcy's Law and the Field Equations of the Flow of Underground Fluids," American Institute of Mining and Metallurgy, Petroleum Engineering Transactions, 207:222-239 (1956).

40. Hutcheon, W. L., "Moisture Flow Induced by Thermal Gradients with Unsaturated Soils," In: Water and Its Conduction in Soils, Highway Research Board, Commission on Physico-Chemical Phenomena in Soils, Special Report No. 40, 113 p. (1958).

41. Kendrick, J. H., "Economic Analysis of a Subsurface Water Pipe Soil Warming System," Chemical Engineering Department Report, University of Arkansas, Fayetteville (1973).

42. Kendrick, J. H., Heat Budget of a Subsurface, Water Pipe, Soil Warming System, M.S.Ch.E. Thesis, University of Arkansas, Fayetteville (1972).

43. Kendrick, J. H., and J. A. Havens, "Heat Transfer Models for a Subsurface, Water Pipe, Soil-Warming System," Journal of Environmental Quality, 2(2):188-196 (1973).

44. King, L. G., "Description of Soil Characterisitics for Partially Saturated Flow," Soil Science Society of America Proceedings, 29:359-362 (1965).

45. Klute, A., F. D. Whisler, and E. J. Scott, "Numerical Solution of the Nonlinear Diffusion Equation for Water Flow in a Horizontal Soil Column of Finite Length," Soil Science Society of America Proceedings, 29:353-358 (1965).

46. Kuzmak J. M., and P. J. Sereda, "The Mechanism by Which Water Moves Through a Porous Material Subjected to a Temperature Gradient, I: Introduction of a Vapor Gap into a Saturated System," Soil Science, 84:291-299 (1957).

47. Kuzmak, J. M., and P. J. Sereda, "The Mechanism by Which Water Moves Through a Porous Material Subjected to a Temperature Gradient, II: Salt Tracer and Streaming Potential to Defect Flow in the Liquid Phase," Soil Science, 84:419-422 (1957).

48. Letey, J., "Movement of Water Through Soil as Influenced by Osmotic Pressure and Temperature Gradients," Hilgardia, 39: 405-418 (1968).

49. Matthes, R. K., and H. D. Bowen, "Steady-State Heat and Moisture Transfer in an Unsaturated Soil," American Society of Agricultural Engineers, Transactions (1968).

50. Miller, E. E., and A. Klute, "Dynamics of Soil Water, I: Mechanical Forces," In: Irrigation of Agricultural Lands, R. M. Hagen, H. R. Haise, and T. W. Edminster, editors, American Society of Agronomy, Monograph No. 11, Madison, Wisconsin (1967).

51. Moore, R. E., "The Relation of Soil Temperature to Soil Moisture, Pressure, Potential, Retention, and Infiltration Rate," Soil Science Society of America Proceedings, 5:61-64 (1940).

52. Perry, R. H., C. H. Chitton, and S. D. Kirkpatrick, Chemical Engineers Handbook, 4th, McGraw-Hill, New York (1963).

53. Peters, M. S., and K. D. Timmerhaus, Plant Design and Economics for Chemical Engineers, 2nd, McGraw-Hill, New York (1968).

54. Philip, J. R., "Physics of Water Movement in Porous Solids," In: Water and Its Conduction in Soils, Highway Research Board, Commission of Physico-Chemical Phenomena in Soils, Special Report No. 40:147-163 (1958).

55. Philip, J. R., "Theory of Infiltration," In: Advances in Hydroscience, V. T. Chow editor, 5:215-296 (1969).

56. Philip, J. R., and D. A. DeVries, "Moisture Movement in Porous Materials Under Temperature Gradients," Transactions, American Geophysical Union, 38(2):222-232 (1957).

57. Prigogine, I., Introduction to Thermodynamics of Irreversible Processes, 3rd, Interscience Publishers, New York (1967).

58. Renfro, G. M., "Applying Water Under the Surface of the Ground," United States Department of Agriculture, 1955 Yearbook:273-278.

59. Robins, J. S., W. O. Pruitt, and W. H. Gardner, "Unsaturated Flow of Water in Field Soils and its Effect on Soil Moisture Investigations," Soil Science Society of America Proceedings, 18:344-347 (1958).

60. Rollins, R. L., M. C. Spangler, and D. Kirkham, "Movement of Soil Moisture Under a Thermal Gradient," National Research Council, Proceedings, Highway Research Board Meeting, 33:492-508 (1954).

61. Rose, C. W., "Water Transport in Soil with a Daily Temperature Wave, II: Analysis," Australian Journal of Soil Research, 6: 45-57 (1968).

62. Rosenberg, N. J., K. W. Brown, T. A. Hales, P. Doraiswamy, and D. W. Sandin, Energy Sources for Evapotranspiration in the Plains Region, Nebraska Water Resources Institute, Horticulture Progress Report No. 73, 153 p. (1969).

63. Royal Dutch/Shell Group of Companies, The Petroleum Handbook, Shell International Petroleum Company Limited, London (1966).

64. Skaggs, R. W., and G. J. Kriz, Water Table Control and Subsurface Irrigation in Mineral and High Organic Coastal Plain Soils, Water Resources Research Institute of the University of North Carolina, Report No. 67, 63 p. (1972).

65. Sliepcevich, C. M., and H. T. Hashemi, "Irreversible Thermodynamics," Chemical Engineering Education, Summer:109-113 (1968).

66. Sonntag, R. E., and G. J. van Wylen, Fundamentals of Classical Thermodynamics, John Wiley and Sons, New York (1968).

67. Sonntag, R. E., and G. J. van Wylen, Fundamentals of Statistical Thermodynamics, John Wiley and Sons, New York (1966).

68. Spanner, D., "The Active Transport of Water Under a Temperature Gradient," Society of Experimental Biology VIII, Active Transport: 76-93 (1954).

69. Taylor, S. A., and J. W. Cary, "Analysis of the Simultaneous Flow of Water and Heat with the Thermodynamics of Irreversible Processes," Transactions, International Congress of Soil Science, 7th, (1):80-90, Madison, Wisconsin (1960).

70. Taylor, S. A., and L. Cavassa, "The Movement of Soil Moisture in Response to Temperature Gradients," Soil Science Society of America Proceedings, 18:351-358 (1954).

71. Treybal, R. E., Mass Transfer Operations, 2nd, McGraw-Hill, New York (1968).

72. Weeks, L. V., S. J. Richards, and J. Letey, "Water and Salt Transfer in Soil Resulting from Thermal Gradients," Soil Science Society of America Proceedings, 32:193-197 (1968).

73. Wei, J., "Irreversible Thermodynamics in Engineering," Industrial and Engineering Chemistry, 58(10):55-60 (1966).

74. Wierenga, P. J., and C. T. DeWit, "Simulation of Heat Transfer in Soils," Soil Science Society of America Proceedings, 34(6): 845-848 (1970).

75. Willis, W. O., H. L. Parkinson, C. W. Carlson, and H. J. Haas, "Water Table Change and Soil Moisture Loss Under Frozen Conditions," Soil Science, 98:244-248 (1964).

76. Winterkorn, H. F., "Mass Transport Phenomena in Moist Porous Systems as Viewed from the Thermodynamics of Irreversible Processes," In: Water and Its Conduction in Soils, Highway Research Board, Commission on Physico-Chemical Phenomena in Soils, Special Report No. 40:324-337 (1958).

77. Woodside, W., and J. M. Kuzmak, "Effect of Temperature Distribution on Moisture Flow in Porous Materials," Transactions, American Geophysical Union, 39:676-680 (1958).

Appendix II

SOIL PROPERTY DATA

The following tables list typical values of the parameters necessary to solve the Cary and Taylor model of coupled heat and moisture transfer in unsaturated soils. Parameters were taken from sources indicated, or calculated from data taken from these sources.

Explanation of Tables

Soil Description

Sand - Percentage of particles in the medium with diameter 0.2-0.02 mm.

Silt - Percentage of particles in the medium with diameter 0.02-0.002 mm.

Clay - Percentage of particles in the medium with diameter < 0.002 mm.

Saturation Moisture Content

Density - Bulk density of the medium, g/cm^3

Porosity

Source - Literature citation

ψ - Matric suction potential, cm of water

D - Coefficient of diffusivity of liquid water in the medium, cm^2/min

λ - Thermal conductivity, Kcal/cm sec°C

$-\beta^*$ - The ratio of the moisture content gradient to the ℓn temperature gradient for a sealed soil column operating at steady state

θ - Volumetric moisture content, cm^3 of water/cm^3 of soil

* - Denotes moisture content on a weight basis, g of water/g of soil

EX - Denotes 10^X (Fortran IV notation).

Table A.II -1. Values of the ratio of the volumetric moisture content gradient to the ln temperature gradient (β^*) in sealed soil columns operating at steady state vs. volumetric moisture content.

		β^*	θ
Soil Description:	Columbia Fine Sandy Loam	3.75	0.03
Sand:	-	1.5	0.085
Silt:	-	12.5	0.12
Clay:	-		
Saturation Moisture Content:	-		
Density:	1.6		
Porosity:	-		
Source:	(17)		
Soil Description: 0.5-1.0 mm.	Palouse Silt Loam, ΔT=15.5°C	1.6	0.055
Sand:	-	2.4	0.059
Silt:	-	4.0	0.065
Clay:	-	13.5	0.085
		35.0	0.11
Saturation Moisture Content:	(?)	35.0	0.16
Density:	1.05	13.5	0.18
Porosity:	-	6.0	0.21
Source:	(18)		
Initial Moisture Content = 0.180			
Soil Description:	See (28)	6.0	0.04
Sand:	-	12.0	0.0675
Silt:	-	22.0	0.0725
Clay:	-	22.0	0.1125
		11.0	0.13
Saturation Moisture Content:	-	6.0	0.145
Density:	2.5-2.6	3.0	0.15
Porosity:	-	0.5	0.16
Source:	(18)		
Soil Description:	Millville Silt Loam	15.5	0.06
Sand:	-	15.5	0.20
Silt:	-		
Clay:	-		
Saturation Moisture Content:	-		
Density:	-		
Porosity:	0.35-0.50		
Source:	(12)		

Table A.II -1 (continued)

		β*	θ
Soil Description: 0.5-1.0 mm.Palouse Silt Loam,ΔT=15°C		2.5	0.060
Sand:	-	12.5	0.080
Silt:	-	21.0	0.100
Clay:	-	27.5	0.105
		35.0	0.110
Saturation Moisture Content:		35.0	0.150
Density:	1.05	19.0	0.170
Porosity:	-	9.5	0.190
Source:	(18)		
Initial Moisture Content = 0.152			
Soil Description: 0.5-1.0 mm.Palouse Silt Loam,ΔT=10°C		2.5	0.070
Sand:	-	6.0	0.080
Silt:	-	23.0	0.100
Clay:	-	32.5	0.150
		32.5	0.155
Saturation Moisture Content:		16.0	0.170
Density:	1.05	5.0	0.190
Porosity:	-		
Source:	(18)		
Initial Moisture Content = 0.180			
Soil Description: 0.5-1.0 mm.Palouse Silt Loam,ΔT=5°C		5.0	0.08
Sand:	-	20.0	0.09
Silt:	-	34.0	0095
Clay:	-	34.0	0.145
		13.0	0.170
Saturation Moisture Content:		7.0	0.190
Density:	1.05		
Porosity:	-		
Source:	(18)		
Initial Moisture Content = 0.180			
Soil Description: 0.5-1.0 mm.Palouse Silt Loam,ΔT=10°C		2.5	0.065
Sand:	-	12.0	0.090
Silt:	-	18.0	0.100
Clay:	-	32.5	0.110
		32.5	0.155
Saturation Moisture Content:	-	15.0	0.18
Density:	-		
Porosity:	1.05		
Source:	(18)		
Initial Moisture Content = 0.152			

Table A.II -1 (continued)

		β*	θ
Soil Description:	0.5-1.0 mm.Palouse Silt Loam,ΔT=5°C	2.0	0.065
Sand:		11.0	0.080
Silt:		20.0	0.100
Clay:		23.0	0.110
		30.0	0.125
Saturation Moisture Content:		30.0	0.150
Density:	1.05	17.5	0.170
Porosity:		10.0	0.180
Source:	(18)		
	Initial Moisture Content = 0.152		

Soil Description:
Sand:
Silt:
Clay:

Saturation Moisture Content:
Density:
Porosity:
Source:

Soil Description:
Sand:
Silt:
Clay:

Saturation Moisture Content:
Density:
Porosity:
Source:

Soil Description:
Sand:
Silt:
Clay:

Saturation Moisture Content:
Density:
Porosity:
Source:

Factors concerning the use of β^*

Units:

From the Cary and Taylor model,

$$\frac{J_w}{\rho} \simeq -D\beta^* \nabla \ell nT$$

where J_w is the flow of moisture, g/cm^2-unit time

D is the coefficient of diffusivity of liquid water in soil, cm^2/unit time

T is temperature, °K

ρ is the density of the system, g/cm^3

∇ is the gradient, 1/cm.

Use of the identity $\nabla \ell nT = -\nabla T/T$

$$\frac{J_w}{\rho} \simeq -D\beta^* \left(-\frac{\nabla T}{T}\right).$$

Substituting units

$$\left[\frac{g}{cm^2\text{-unit time}}\right]\left[\frac{cm^3}{g}\right] = \left[\frac{cm^2}{\text{unit time}}\right]\beta^*\left[\frac{°K/cm}{°K}\right].$$

β^* is now seen to be dimensionless. The data of Cassel et al. [17] are presented by the authors as 1/ℓn°K. The data of Gee [18] are presented by the author as 1/°K, although this perhaps should be 1/ℓn°K. The numerical values of the data of Cassel et al. (17) and Gee (18), however, are correct as presented in Table A. II-1.

Effect of Temperature:

β^* appears to be only a weak function of temperature.

Table A. II -2. Values of thermal conductivity in Kcal/cm sec°C vs. volumetric moisture content.

		λ	θ
Soil Description:	Quincy Sand at 25°C	0.7	0.05
Sand:	90	0.9	0.10
Silt:	6	1.4	0.15
Clay:	4	2.2	0.20
		2.7	0.25
Saturation Moisture Content:	0.48	3.2	0.30
Density:	-	3.5	0.35
Porosity:	-	4.0	0.40
Source:	(24)	4.2	0.45
Soil Description:	Quincy Sand at 45°C	1.0	0.05
Sand:	90	1.8	0.10
Silt:	6	2.5	0.15
Clay:	4	3.0	0.20
		3.4	0.25
Saturation Moisture Content:	0.48	3.8	0.30
Density:	-	4.0	0.35
Porosity:	-	4.2	0.40
Source:	(24)		
Soil Description:	Cloquato Loam at 25°C	0.5	0.05
Sand:	43	0.5	0.10
Silt:	37	0.5	0.15
Clay:	20	0.9	0.20
		1.5	0.25
Saturation Moisture Content:	0.62	1.8	0.30
Density:	-	2.0	0.35
Porosity:	-	2.2	0.40
Source:	(24)	2.3	0.45
		2.4	0.50
		2.5	0.55
		2.5	0.60
Soil Description:	Cloquato Loam at 45°C	0.6	0.05
Sand:	43	0.8	0.10
Silt:	37	1.3	0.15
Clay:	20	1.8	0.20
		2.0	0.25
Saturation Moisture Content:	0.62	2.1	0.30
Density:	-	2.2	0.35
Porosity:	-	2.3	0.40
Source:	(24)	2.4	0.45
		2.5	0.50
		2.6	0.55
		2.6	0.60

Table A.II -2 (continued)

		λ	θ
Soil Description:	-	0.5	0.00
Sand:	-	2.0	0.10
Silt:	-	2.5	0.15
Clay:	-	3.0	0.25
		3.5	0.35
Saturation Moisture Content:	-	4.0	0.50
Density:	-		
Porosity:	-		
Source:	(29)		
Soil Description:	-	0.074	dry
Sand:	-	3.73	wet
Silt:	-		
Clay:	-		
Saturation Moisture Content:	-		
Density:	-		
Porosity:	-		
Source:	(25)		
Soil Description:	Sandy	0.66	0.022
Sand:	-	0.90	0.033
Silt:	-	1.20	0.05
Clay:	-	1.63	0.10
		1.86	0.15
Saturation Moisture Content:	-	2.02	0.20
Density:	-		
Porosity:	-		
Source:	(19)		
Soil Description:	Clayey	0.30	0.10
Sand:	-	0.72	0.20
Silt:	-	1.14	0.30
Clay:	-	1.56	0.40
Saturation Moisture Content:	-		
Density:	-		
Porosity:	-		
Source:	(19)		

Table A.II -3. Values of the coefficient of diffusivity for liquid water in soil in cm^2/min vs. volumetric moisture content (* denotes moisture content on a weight basis).

		D	θ
Soil Description:	Traver Sandy Loam	0.005	0.05*
Sand:	52	0.04	0.10
Silt:	39	0.20	0.15
Clay:	9	2.0	0.20
		10.0	0.25
Saturation Moisture Content:	0.28*	50.0	0.28
Density:	1.4-1.5		
Porosity:	-		
Source:	(30)		
Soil Description:	Indio Loam	0.003	0.05*
Sand:	33	0.01	0.10
Silt:	51	0.03	0.15
Clay:	16	0.08	0.20
		0.70	0.30
Saturation Moisture Content:	0.45*	2.0	0.35
Density:	-	6.0	0.40
Porosity:	1.3-1.4	18.0	0.45
Source:	(30)		
Soil Description:	Chino Clay	0.0005	0.05*
Sand:	11	0.0012	0.10
Silt:	34	0.003	0.15
Clay:	55	0.008	0.20
		0.02	0.25
Saturation Moisture Content:	0.62*	0.04	0.30
Density:	1.2-1.3	0.10	0.35
		0.20	0.40
Source:	(30)	0.50	0.45
		1.2	0.50
		3.0	0.55
		7.0	0.60
Soil Description:	Yolo Loam	0.002	0.05*
Sand:	38	0.006	0.10
Silt:	39	0.02	0.15
Clay:	23	0.06	0.20
		0.25	0.25
Saturation Moisture Content:	0.42*	0.70	0.30
Density:	1.25-1.35	2.5	0.35
Porosity:	-	7.0	0.40
Source:	(30)		

Table A.II -3 (continued)

		D	θ
Soil Description:	Medium Sand at 20°C	0.06	0.05
Sand:	-	0.16	0.10
Silt:	-	0.32	0.20
Clay:	-	1.0	0.30
		1.6	0.35
Saturation Moisture Content:	0.425	10.0	0.40
Density:	-		
Porosity:	-		
Source:	(31)		
Soil Description:	Webster Silty Clay Loam	0.01	0.00
Sand:	19.9	0.02	0.05
Silt:	48.0	0.03	0.10
Clay:	32.1	0.05	0.15
		0.07	0.20
Saturation Moisture Content:	0.52	0.10	0.25
Density:	1.2	0.30	0.30
Porosity:	-	1.0	0.35
Source:	(16)	7.0	0.40
		12.0	0.45
Soil Description:	Pachappa Sandy Loam	0.007	0.05*
Sand:	59	0.028	0.10
Silt:	33	0.080	0.15
Clay:	8	0.350	0.20
		1.4	0.25
Saturation Moisture Content:	0.35*	4.9	0.30
Density:	1.4-1.5		
Porosity:	-		
Source:	(32)		
Soil Description:	Pachappa Sandy Loam	0.007	0.05*
Sand:	59	0.03	0.10
Silt:	33	0.10	0.15
Clay:	8	0.50	0.20
		1.5	0.25
Saturation Moisture Content:	0.35*	6.0	0.30
Density:	1.4-1.5	20.0	0.35
Porosity:	-		
Source:	(30)		

Table A. II-3 (continued)

		D	θ
Soil Description:	Sarpy Loam		
Sand:			
Silt:			
Clay:			
Saturation Moisture Content:			
Density:			
Porosity:			
Source:	(33) $D = 7.45 \times 10^{-3} e^{19.78\theta}$		
Soil Description:	Fort Collins Silty Clay Loam		
Sand:			
Silt:			
Clay:			
Saturation Moisture Content:			
Density:			
Porosity:			
Source:	(34) $D = 9.53 \times 10^{-2} e^{17.83\theta}$		
Soil Description:	Loamy Sand	0.1	0.08*
Sand:	73.5	2.0	0.12
Silt:	15.0	5.0	0.16
Clay:	11.5	20.0	0.20
		50.0	0.24
Saturation Moisture Content:	0.28*		
Density:	1.4-1.6		
Porosity:	0.4-0.5		
Source:	(35)		
Soil Description:	0.25-0.5 mm Sand	0.032	0.010*
Sand:	-	0.661	0.015
Silt:	-	2.2	0.021
Clay:	-	4.7	0.031
		8.0	0.043
Saturation Moisture Content:	0.375*	11.3	0.055
Density:	-	19.4	0.070
Porosity:	-	32.2	0.095
Source:	(36)	43.2	0.125
		48.1	0.165
		82.2	0.235
		157	0.300
		696	0.320
		1000	0.330
		3774	0.352

Table A. II -3 (continued)

		D	θ
Soil Description:	Yolo Light Clay		
Sand:	23.8		
Silt:	45.0		
Clay:	31.2		
Saturation Moisture Content:	0.495		
Density:	1.32		
Porosity:	-		
Source:	(37) $D = 3.75 \times 10^{-6} e^{32\theta *}$		
Soil Description:	Pachappa Loam		
Sand:	-		
Silt:	-		
Clay:	-		
Saturation Moisture Content:	0.33		
Density:	1.42		
Porosity:	-		
Source:	(37) $D = 1.248 \times 10^{-3} e^{27.8\theta *}$		
Soil Description:	Momona Silt Loam	0.10	0.305
Sand:	-	25.0	0.455
Silt:	-		
Clay:	-		
Saturation Moisture Content:	0.455		
Density:	-		
Porosity:	-		
Source:	(38)		
Soil Description:	Ida Silt Loam	0 .25	0.28
Sand:	-	25.0	0.47
Silt:	-		
Clay:	-		
Saturation Moisture Content:	0.47		
Density:	-		
Porosity:	-		
Source:	(38)		

Factors concerning the use of D

Hanks and Bowers (33) and Hanks and Gardner (34) demonstrated that a wide variance in the numerical value of D will not appreciably affect the flow of moisture except at regions near saturation. This relation has not been determined for the case of coupled moisture and heat flow and due caution of D therefore must be exercised as to the accuracy.

Gardner (32) showed that D is not a strong function of temperature except at regions near saturation or with very dry conditions.

Table A.II -4. Values of the matric suction potential in cm vs. volumetric moisture content (* denotes moisture content on a weight basis.

		-ψ	θ
Soil Description:	Yolo Fine Sandy Loam	250	0.20
Sand:	50.8	200	0.22
Silt:	31.5	150	0.25
Clay:	17.7	100	0.32
		50	0.36
Saturation Moisture Content:	0.4		
Density:	1.28		
Porosity:	-		
Source:	(39)		
Soil Description:	Medium Sandy at 20°C	100	0.025
Sand:	-	30	0.10
Silt:	-	30	0.40
Clay:	-		
Saturation Moisture Content:	0.425		
Density:	-		
Porosity:	-		
Source:	(31)		
Soil Description:	Webster Silty Clay Loam	4.0E5	0.10
Sand:	19.9	70000	0.15
Silt:	48.0	15000	0.20
Clay:	32.1	5000	0.25
		1500	0.30
Saturation Moisture Content:	0.52	700	0.35
Density:	1.2	300	0.40
Porosity:	-	150	0.45
Source:	(16)	80	0.50
Soil Description:	Urrbrae Loam	2.5E5	0.025
Sand:	52.1	30000	0.05
Silt:	31.3	10000	0.075
Clay:	16.6	2500	0.10
		1800	0.125
Saturation Moisture Content:	0.24	1500	0.15
Density:	1.4-1.6	450	0.20
Porosity:	-	300	0.225
Source:	(40)		

Table A.II -4 (continued)

		-ψ	θ
Soil Description:	Oakley Sand	450	0.03
Sand:	90.9	400	0.04
Silt:	3.5	80	0.05
Clay:	5.6	60	0.06
		40	0.09
Saturation Moisture Content:	0.29	20	0.14
Density:	1.48	10	0.20
Porosity:	-	5	0.25
Source:	(41)	0	0.29
Soil Description:	Yolo Fine Sandy Loam	290	0.15
Sand:	50.8	200	0.16
Silt:	31.5	150	0.17
Clay:	17.7	130	0.18
		110	0.19
Saturation Moisture Content:	0.40	100	0.20
Density:	1.28	80	0.22
Porosity:	-	50	0.28
Source:	(41)	10	0.35
Soil Description:	Yolo Light Clay	600	0.18
Sand:	23.8	400	0.19
Silt:	45.0	340	0.20
Clay:	31.2	280	0.21
		220	0.22
Saturation Moisture Content:	0.495	160	0.23
Density:	1.32	140	0.24
Porosity:	-	80	0.27
Source:	(41)	50	0.30
		20	0.35
Soil Description:	Palouse Silt Loam	1.0E6	0.025
Sand:	-	5.0E5	0.040
Silt:	-	2.0E5	0.045
Clay:	-	1.0E5	0.050
		50000	0.070
Saturation Moisture Content:	-	20000	0.085
Density:	1.05	10000	0.100
Porosity:	-	5000	0.135
Source:	(18)	2000	0.165
		1000	0.185
		500	0.215
		200	0.235
		100	0.260
		50	0.310
		20	0.360
		10	0.430

Table A.II -4 (continued)

		$-\psi$	θ
Soil Description:	Yolo Light Clay	18000	0.08
Sand:	23.8	4000	0.15
Silt:	45.0	1200	0.20
Clay:	31.2	400	0.25
		180	0.30
Saturation Moisture Content:	0.495	100	0.34
Density:	1.32	40	0.42
Porosity:	-	20	0.46
Source:	(42)	12	0.48
Soil Description:	Lumbec Sandy Loam	280	0.30
Sand:	-	160	0.32
Silt:	-	80	0.35
Clay:	-	40	0.40
		20	0.43
Saturation Moisture Content:	0.46		
Density:	-		
Porosity:	-		
Source:	(37)		
Soil Description:	Panoche Clay Loam at 15 cm	150	0.35
Sand:	- depth	70	0.375
Silt:	-	40	0.40
Clay:	-	8	0.425
Saturation Moisture Content:	-		
Density:	-		
Porosity:	-		
Source:	(43)		
Soil Description:	Yolo Light Clay	592	0.238
Sand:	23.8	440	0.251
Silt:	45.0	366	0.264
Clay:	31.2	278	0.277
		224	0.290
Saturation Moisture Content:	-	172	0.304
Density:	0.495	140	0.317
Porosity:	-	108	0.330
Source:	(44)	67	0.370
		50	0.396
		37	0.422
		27	0.449
		16	0.475
		8	0.488

Table A.II -4 (continued)

		-ψ	θ
Soil Description:	0.25-0.5mm Sand	60	0.010*
Sand:	1	52	0.014
Silt:	-	46	0.019
Clay:	-	40	0.028
		36	0.036
Saturation Moisture Content:	0.357*	32	0.055
Density:	-	28	0.095
Porosity:	-	26	0.125
Source:	(45)	24	0.165
		22	0.235
		20	0.300
		10	0.348
		0	0.357
Soil Description:	104-109μ Sand at 4°C	62	0.32
Sand:	-	65	0.24
Silt:	-	70	0.16
Clay:	-	80	0.12
		95	0.08
Saturation Moisture Content:	0.37	150	0.04
Density:	1.64		
Porosity:	-		
Source:	(46)		
Soil Description:	53-74μ Sand at 4°C	160	0.32
Sand:	-	165	0.28
Silt:	-	170	0.24
Clay:	-	175	0.20
		180	0.16
Saturation Moisture Content:	0.38	195	0.12
Density:	1.64	230	0.08
Porosity:	-		
Source:	(46)		
Soil Description:	13.0-18.5μ Sand at 4°C	625	0.40
Sand:	-	690	0.32
Silt:	-	730	0.24
Clay:	-	800	0.16
		1000	0.12
Saturation Moisture Content:	0.44	1200	0.09
Density:	1.46		
Porosity:	-		
Source:	(46)		

Table A.II -4 (continued)

		-ψ	θ
Soil Description:	Loamy Sand	6000	0.04*
Sand:	73.5	2000	0.08
Silt:	15.0	200	0.12
Clay:	11.5	100	0.16
		60	0.20
Saturation Moisture Content:	.28*	20	0.24
Density:	1.4-1.6	1	0.28
Porosity:	0.4-0.5		
Source:	(35)		
Soil Description:	104-109μ Sand at 44°C	52	0.32
Sand:	-	55	0.24
Silt:	-	60	0.16
Clay:	-	70	0.12
		75	0.08
Saturation Moisture Content:	0.37	125	0.04
Density:	1.64		
Porosity:	-		
Source:	(46)		
Soil Description:	53-74μ Sand at 44°C	140	0.32
Sand:	-	145	0.28
Silt:	-	150	0.24
Clay:	-	155	0.20
		160	0.16
Saturation Moisture Content:	0.38	175	0.12
Density:	1.64	200	0.08
Porosity:	-		
Source:	(46)		
Soil Description:	13.0-18.5μ Sand at 44°C	525	0.40
Sand:	-	590	0.32
Silt:	-	630	0.24
Clay:	-	700	0.16
		900	0.12
Saturation Moisture Content:	0.44	1100	0.09
Density:	1.46		
Porosity:	-		
Source:	(46)		

Factors concerning the use of ψ

It has been shown that the Cary and Taylor model parameter β can be related to ψ by

$$\beta = \beta^* \frac{\partial \psi}{\partial \theta}$$

where $-\beta$ is the ratio of the chemical potential gradient to the ℓn temperature gradient, cal/g

$-\beta^*$ is the ratio of the volumetric moisture content gradient to the ℓn temperature gradient, dimensionless

θ is the volumetric moisture content, cm^3 of water/cm^3 of soil.

ψ can be seen to have the units of cal/g. To convert ψ from cm of water to cal/g use the relation

$$[\text{cm of water}] \left[\frac{1 \text{ atm}}{1033 \text{ cm of water}}\right] \left[\frac{1 \text{ cal}}{41.29 \text{ cm}^3\text{-atm}}\right] \left[\frac{\text{cm}^3}{\text{g}}\right]$$

where the last term is one over the density of the system in g/cm^3.

Moore (47) and Wilkinson and Klute (46) have shown that ψ is not a strong function of temperature. Furthermore, a comparison of the data of Wilkinson and Klute (46) indicates that $\partial\psi/\partial\theta$ is nearly constant for temperatures of 4°C and 44°C.